PERGAMON

Journal of Structural Geology 25 (2003) 135–158

JOURNAL OF STRUCTURAL GEOLOGY

www.elsevier.com/locate/jsg

Geometric and morphologic evolution of normal fault planes and traces from 2D to 4D data

Denis Marchal[a,*], Michel Guiraud[b], Thierry Rives[c]

[a]*I.F.P., 1 & 4 av. Bois-Préau, 92852 Rueil-Malmaison, France*
[b]*Université de Bourgogne, Centre des Sciences de la Terre, UMR 5561, 6 bvd Gabriel, 21000 Dijon, France*
[c]*Elf Exploration-Production, CSTJF, Av. Larribau, 64018 Pau cedex, France*

Received 20 December 1999; accepted 17 October 2001

Abstract

The detailed 3D geometry of normal fault planes is described and analysed using datasets from outcrop studies (2D), seismic surveys (3D) and analogue models (4D). Different geometric configurations of simple isolated normal faults are studied by reference to processes of normal fault propagation. When a normal fault propagates without interacting with other fault zones, the entire border of the principal plane displays characteristic connected secondary structures. These secondary structures cause bifurcations of the principal fault terminations. The along-strike terminations of the principal plane display typical bifurcation configurations ('ear geometry'). The orientation of the bifurcations depends on the vertical direction of propagation (downwards and/or upwards). The along-dip terminations display en échelon secondary fault planes linked to the principal plane and are described as 'lobate geometry'. A 3D genetic model of isolated normal fault geometry is proposed with a new general terminology for the secondary structures. When two isolated normal faults propagate towards each other and overlap, the two principal planes connect up via a relay fault. The resulting geometry is a longer fault exhibiting a characteristic undulation with two inactive branches.

Keywords: Normal fault; Geometry; Termination; Bifurcation; Propagation

1. Introduction

Segmented normal faults are observed in all extensional domains worldwide across a broad range of scales: centimetre-scale (Laubach et al., 1992; Schlische et al., 1996), metre-scale (Peacock and Sanderson, 1991, 1994; Childs et al., 1996a; Willemse, 1997), and kilometre-scale (Trudgill and Cartwright, 1994; Childs et al., 1995, 1996b; Cowie and Shipton, 1998; Crider and Pollard, 1998). In hydrocarbon exploration and production, complex normal fault networks play an important role in creating hydrocarbon traps and migration pathways (e.g. Morley et al., 1990). Better knowledge of individual fault plane geometry should help in unravelling the more complex geometries and thus provides a more accurate interpretation of hydrocarbon traps. Similarly, normal faults can control structures used to store hydrocarbons (e.g. Dreyer, 1982). Thorough knowledge of the 3D geometry of fault terminations enables better evaluation of the sealing potential of a fault zone. Normal fault systems in continental rifts and extensional areas are important triggers of powerful and destructive earthquakes (Bruhn and Schultz, 1996; Yeats et al., 1997). Active normal fault planes very often appear as segmented structures (Jackson and White, 1989) and segment boundaries play a fundamental role in the initiation and termination of earthquakes ruptures (De Polo et al., 1991; Machette et al., 1991).

Published material on normal fault geometries falls into two broad categories: (i) 2D studies of fault trace geometry, and (ii) 3D studies of normal fault plane geometry. A review of the literature shows that normal fault geometries range from simple to highly complex. The increasing complexity of the fault plane network defining the fault zone is often correlated with increasing resolution of the tools used to study the fault zone (e.g. Knipe et al., 1998). A simple fault plane appears to be elliptical under low resolution (e.g. Nicol et al., 1996) but can be subdivided into a principal plane with numerous secondary planes under high resolution (e.g. McGrath and Davison, 1995). While such works have furthered understanding of normal fault plane geometry many points are still debated or left unexplored.

The purposes of this study are (1) to detail the 3D geometry of normal faults and (2) to explain the characteristics of

* Corresponding author. Now at: Perez Companc de Venezuela, Caracas, Venezuela.
E-mail address: dmarchal@pecom.com.ve (D. Marchal).

0191-8141/02/$ - see front matter
PII: S0191-8141(02)00011-1

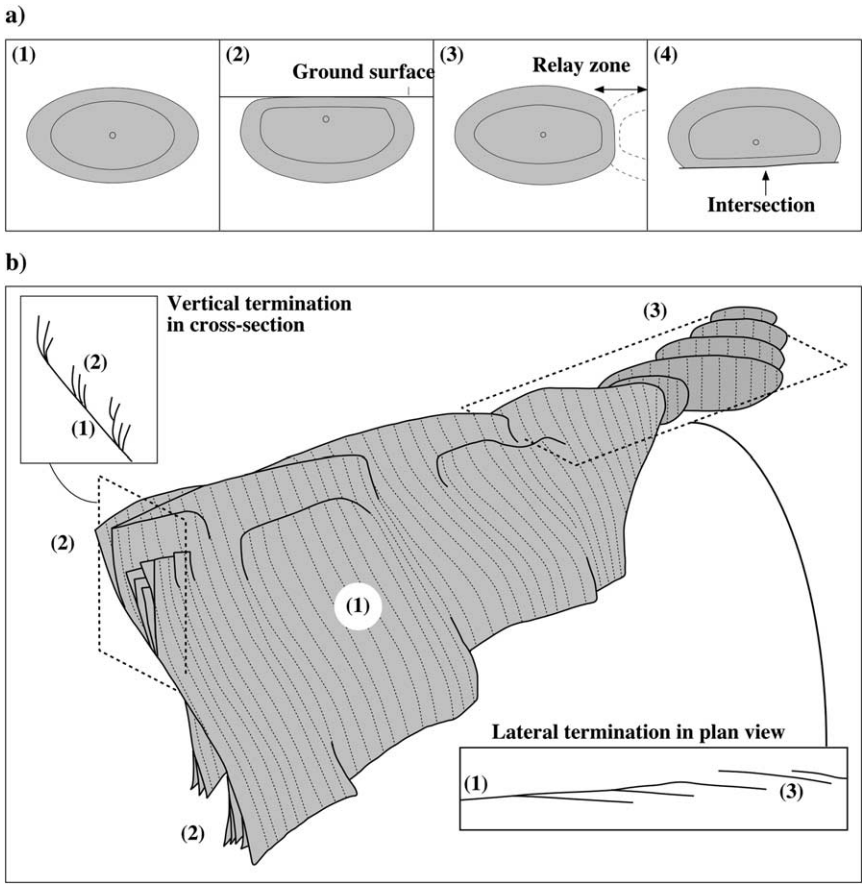

Fig. 1. Simplified 3D geometry of normal faults. (a) Variations in normal fault shape. The simplest shape for a blind normal fault is an elliptical plane (1). Fault shape may be affected by interaction with other features: restriction by the ground surface (2); overlap with another fault plane forming a relay zone (3); intersection with another fault plane (4). These three basic patterns may combine to form complex fault shapes. Modified from Nicol et al. (1996). (b) The half-plane of a normal fault composed of a principal plane (1); branched secondary fault planes at the vertical termination (2); en échelon secondary fault planes at the lateral termination (3). Modified from McGrath and Davison (1995).

normal fault plane morphology. We define 3D geometry as the general shape of the fault plane (including the principal fault plane and the connected secondary fault planes) and morphology as the geometric variations along dip and strike directions of the plane itself. The evolution of a fault zone is related to the propagation processes that lead to the observed geometry. The characteristics of the different normal fault propagation processes are briefly reviewed here and the implications for fault geometry highlighted. To make the results of this study as general as possible, we have deliberately selected examples of normal faults in various extensional tectonic settings, at various scales and including 2D, 3D and 4D datasets. Often, the data used for studying fault geometry are 2D (e.g. field-, remote sensing-, 2D seismic-studies). And even where 3D data is available, it is often studied in 2D only (map- or cross-section-displays). Therefore it is important to be able to decipher fault traces on 2D documents.

The example of the Oklo fault network (Gabon) allows analysis in detail of the fault traces. Datasets from 3D seismic surveys allow direct analysis of the 3D geometry of normal faults. Secondary structures located on the border of normal fault planes are often ignored, even though in some cases they can be imaged. We illustrate the detailed geometry and morphology of isolated normal fault planes. To clearly understand the present geometry of a normal fault or to predict the evolution of the fault zone, we must study the development of such faults over time. Analogue modelling is performed and imaged by X-ray tomography allowing a direct 4D analysis of the spatio-temporal evolution of normal faults. In this study, we present two basic types of 4D propagation sequences, which are representative of two general configurations of normal fault. Finally, on the basis of the natural examples and the analogue modelling presented in this paper, we propose a detailed 3D model of isolated normal fault geometry.

2. Geometry of normal faults: state of the art

There have been many studies of normal fault geometry (e.g. Hancock et al., 1991; Roberts et al., 1991). They indicate that 2D and 3D normal fault geometry may be very

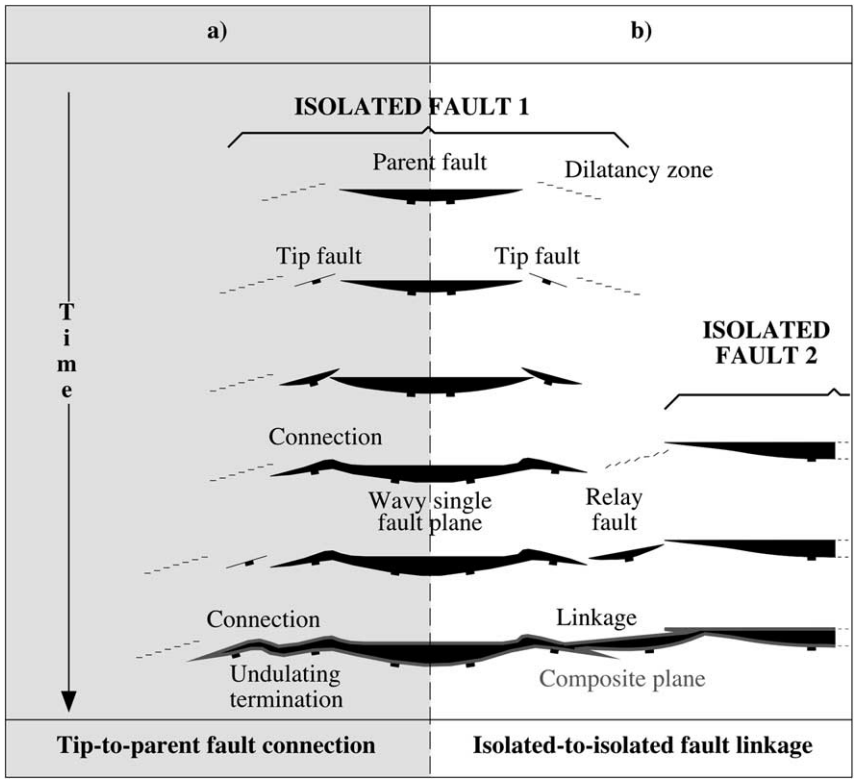

Fig. 2. Isolated normal fault propagation processes (from Marchal et al., 1998). (a) Tip-to-parent fault connection, and (b) isolated-to-isolated fault linkage. See text for details.

complex. However, a number of general characteristics can be mentioned.

2.1. 2D geometries

Several authors have studied normal fault geometry by analysing fault traces on vertical sections (Faure and Chermette, 1989; Vendeville, 1991; Peacock and Zhang, 1994; Childs et al., 1996a). These works show that vertical traces of normal faults vary significantly; from a single ramp to a combination of several ramp-flat pairs. The sudden switch or gradual transition from a ramp to a flat also distinguishes vertically planar faults (Mansfield and Cartwright, 1996) from listric faults (Shelton, 1984). Some authors have also reported that normal fault vertical traces may be discontinuous and composed of segments arranged en échelon (Peacock and Zhang, 1994; Childs et al., 1996a).

In plan view, normal fault trace geometry also shows very wide variability. The horizontal fault traces may be straight or arcuate with various curvatures: concave, convex or complex (Doust and Omatsola, 1990; Machette et al., 1991; Trudgill and Cartwright, 1994; Wu and Bruhn, 1994). Arcuate or straight, the fault traces also often display secondary curvature zones when studied in detail. Different terminologies have been adopted to characterise these secondary structures: bends (e.g. Childs et al., 1995), jogs (e.g. Willemse, 1997) or undulations (Marchal et al., 1998), wherein these features correspond to rapid changes in fault strike direction. Many studies have also shown the segmented nature of horizontal fault traces at different scales (e.g. Morley et al., 1990; Zhang et al., 1991; Trudgill and Cartwright, 1994).

2.2. 3D geometries

2.2.1. Principal plane

Because of the different investigative techniques employed, knowledge of normal fault geometry relates primarily to the ramp part, the flat part being generally poorly defined. Many geologists agree that simple normal fault planes (with a single ramp) may be schematically depicted by a more or less elliptical surface whose longest axis is usually subhorizontal (Rippon, 1985; Barnett et al., 1987; Walsh and Watterson, 1989; Mansfield and Cartwright, 1996; Nicol et al., 1996; Willemse et al., 1996) (Fig. 1a). This idealised fault plane configuration may change as the fault interacts with other faults producing more complex geometries (Needham et al., 1996; Nicol et al., 1996) (Fig. 1a). Several authors also have shown that some structural complexities can affect the principal fault plane: (i) step-up and step-down zones (Stewart and Hancock, 1991), (ii) relay zones forming horses (Huggins et al., 1995), (iii) asperity bifurcations (Childs et al., 1996b) or bends (e.g. Peacock and Zhang, 1994), which are local refractions of the fault plane across lithological layering producing horizontal undulations, and (iv) mega-corrugations (Hancock

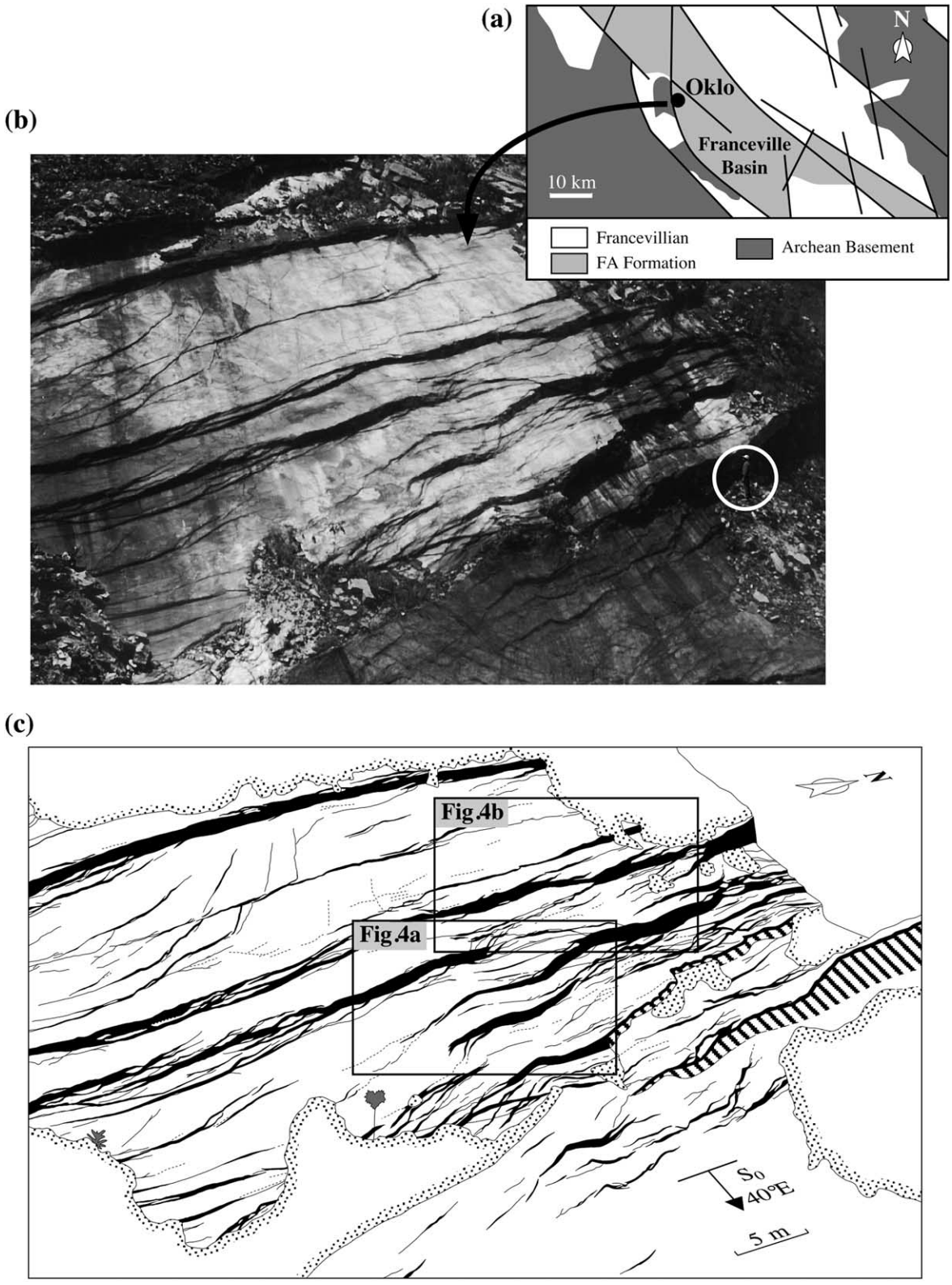

Fig. 3. Traces of normal faults in Oklo Quarry. (a) Location map of the Oklo quarry in the Franceville Basin (S.E. Gabon) (modified from Gauthier-Lafaye and Weber, 1989), (b) Photograph of normal fault traces offsetting bedding surfaces. A geologist is circled for scale. (c) Line drawing of the photograph. Normal fault traces (i.e. fault offsets) are shown in black. Normal faults strike NW–SE to NNW–SSE and dip ENE. Areas masked by vegetation or fallen rocks are stippled and hatched. Boxes outline the areas detailed in Fig. 4.

and Barka, 1987; Needham et al., 1996) which produce subvertical undulations.

2.2.2. Secondary structures

Many secondary structures are associated with the principal plane of the fault. These are preferentially located at the fault terminations. McGrath and Davison (1995) distinguish two principal types of normal fault secondary structures: (i) branched structures and (ii) en échelon structures (Fig. 1b). The branched structures are mainly located at the vertical terminations of the fault plane (Shelton, 1984; Hancock and Barka, 1987; Stewart and Hancock, 1991; Walsh and Watterson, 1991; Gross et al., 1997). These structures are invariably shown connecting up with the principal plane. En échelon structures, mostly described at the horizontal terminations (Wu and Bruhn, 1994; Antonellini and Aydin, 1995; Huggins, 1996), may also be observed in the extension of the vertical terminations (Etchecopar et al., 1986; Childs et al., 1995; Huggins, 1996). When studied in 2D, en échelon faults rarely display connected traces in the principal plane (Griffith, 1980; McGrath and Davison, 1995; Schlische et al., 1996; Cartwright and Mansfield, 1998). Conversely, 3D analysis of these structures often shows their connection with the principal fault (Etchecopar et al., 1986; Childs et al., 1996b).

2.3. Normal fault propagation processes

Using geological data, most workers use the present geometry to depict the propagation processes (Childs et al., 1996b; Cartwright and Mansfield, 1998). However, it has been demonstrated using 4D analogue modelling that our understanding of the 3D geometries of normal faults is dependent on what we know about the propagation processes responsible for the studied fault planes (Marchal et al., 1998). In a previous paper (Marchal et al., 1998), we studied in detail the different processes occurring in normal fault propagation (Fig. 2). The different characteristics of fault propagation occurring in analogue models have been synthesised in a conceptual model, which has been compared with natural geological data and discussed with regard to earlier models of fault growth (i.e. Cowie and Scholz, 1992; Cartwright et al., 1995).

The model involves propagation processes occurring at two different levels of organisation with regard to the fault planes. A normal fault zone is organised in a hierarchical manner into: (1) the single isolated fault system including a principal fault plane (parent fault) and secondary fault planes (tip faults), and (2) the isolated fault set system, which displays clearly different principal fault planes i.e. several soft- or hard-linked single isolated fault systems. At a given scale, the model shows three principal processes of propagation:

1. Radial propagation, or propagation of the fault in its own planes and results in fault lengthening by tip rupture (as defined by Cowie and Scholz, 1992);
2. Tip-to-parent fault connection leads the single isolated fault system to grow by addition of secondary structures (i.e. tip faults) to the principal plane (Marchal et al., 1998) (Fig. 2a);
3. Isolated-to-isolated fault linkage causes two (or several) single isolated fault systems to connect each other via a brittle relay structure (segment linkage in Cartwright et al., 1995) (Fig. 2b).

In normal fault propagation, the three above processes occur alternately over time in various combinations (Marchal et al., 1998).

These three types of process are described for horizontal propagation. Some authors assume that linkage of large segments also occurs for vertical propagation (Mansfield and Cartwright, 1996). A similar conclusion can be drawn for faults developed in brittle/ductile analogue experiments (Marchal et al., 1998). The geometries of 2D fault traces are more numerous than those established in 3D reconstructions. Do normal faults really have such geometric variability or is this variabily induced by the different 2D views of a 3D object displaying complex geometry? The analysis of the datasets presented in this paper goes towards answering this question.

3. 2D analysis of natural normal faults: geometry of the fault traces from the normal fault network of Oklo Quarry, SE Gabon

3.1. Geological setting

A well-preserved normal fault trace network is exposed in Oklo Quarry, south east Gabon. Oklo Quarry is located on the western edge of the Franceville Basin (Fig. 3a). This intracratonic extensional basin (early Proterozoic, 2 Ga) is bounded by major NW–SE normal faults (Gauthier-Lafaye, 1986). The general structure is a graben 60 km long and 30 km wide (Fig. 3a). Reverse and strike-slip faults are also observed and associated with folds characterised by steeply dipping axes (Gauthier-Lafaye, 1986; Gauthier-Lafaye and Weber, 1989). Gauthier-Lafaye and Weber (1989) report that two main phases of deformation generated the tectonic structures bounding and affecting the basin: first, an extension phase causing the basin to collapse and second, a superimposed compressional strike-slip phase. In Oklo Quarry, compressional or strike-slip structures have not been observed inside the studied area. Therefore, it is assumed that the studied normal faults are located in an intact block and are not affected by the subsequent compressional deformation.

The uranium-bearing site at Oklo is located on a near N–S fault zone. The Oklo Quarry contains a 500-m-long exposure of a large structural surface titled 40° eastwards. To the south of the quarry, a gently folded monocline exhibits a

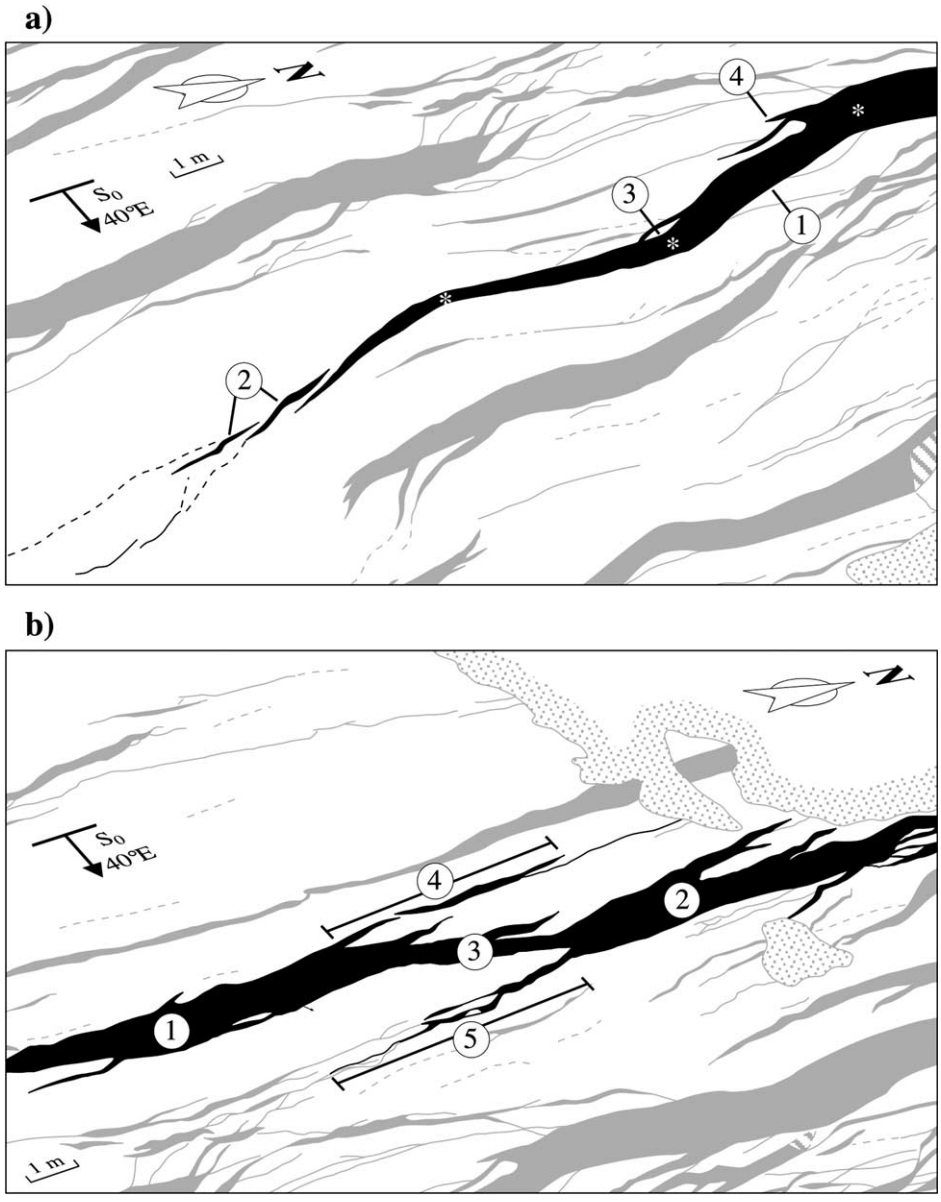

Fig. 4. Detailed normal fault trace geometries (Oklo Quarry). The studied fault traces are in black, the others are in grey. (a) Line drawing of undulating fault traces around the tip of an isolated normal fault. En échelon secondary fault traces (2, tip faults) are located at the end of the major fault trace (1, parent fault). Three bends (marked by white asterisks) are visible along the major fault trace. Two characteristic structures are located in the vicinity of these bends: a small breached relay ramp (3) and splay branches (4). (b) Line drawing of two overlapping faults traces (1 and 2) connected by a relay fault trace (3). The overlaps (4 and 5) are branches with small throw values. The termination (4) displays a typical geometry (secondary fault trace at the tip of the major one) showing that it was previously an isolated fault termination.

network of remarkably well preserved normal faults (Fig. 3b).

3.2. Geometry of normal fault traces

The structural surface studied presents the traces of many normal faults. The well developed faults have throws in the metre range. These faults strike NNW–SSE and dip to the ENE (Fig. 3c). The geometry of these fault traces display complex interrelationships. We mapped the fault traces on the base of a photomosaic of the structural surface. The photos are taken from the opposite side of the exposure.

3.2.1. Isolated normal faults

The termination of a normal fault with maximum exposed throw to the order of 1 m is illustrated in Fig. 4a. Two types of feature must be differentiated: the principal fault trace and the secondary fault traces.

The trace of the principal fault termination (1; Fig. 4a) displays undulations and is defined by three main points of inflexion. Different secondary structures are located at these

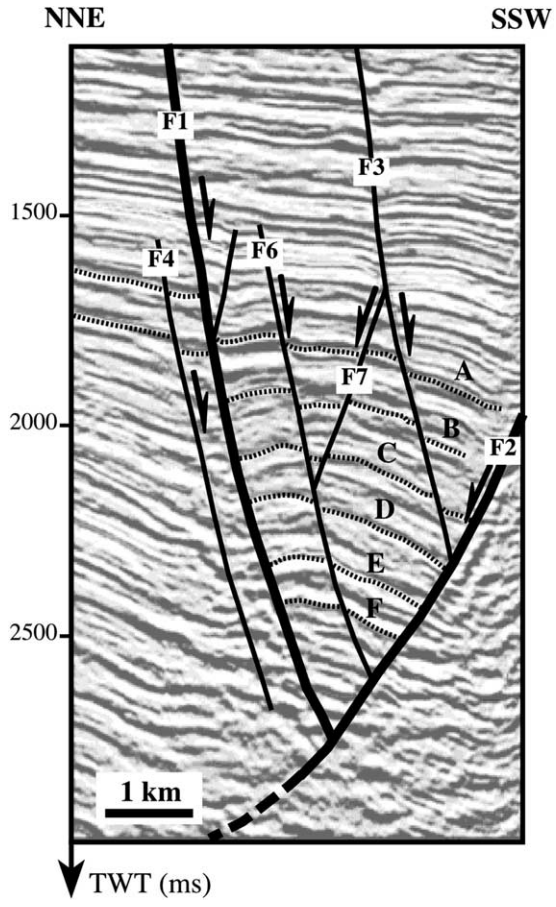

Fig. 5. Seismic section showing major growth faults with the associated collapsed rollover (Niger Delta). The rollover is bounded by synthetic (F2) and antithetic (F1) growth faults and is affected by a set of smaller synthetic and antithetic normal faults (F3, F4, F6 and F7). Structural maps of the six chosen horizons (A to F) are presented in Fig. 6.

points: a relay ramp fractured at both tips ('fault-bounded horse' *sensu* Peacock and Sanderson, 1994) (3; Fig. 4a) and two minor fault traces which splay out from the principal trace (4; Fig. 4a). The secondary fault traces are represented by two small sigmoidal traces (2; Fig. 4a) extending from the principal fault termination. These overlapping fault traces are arranged in a right-stepping en échelon pattern and form a relay ramp between the two secondary traces. The overlapping system formed by the principal fault termination and the secondary faults also displays a relay ramp.

The set formed by the principal fault and the secondary faults is characteristic of an isolated normal fault horizontal termination and perfectly reflects the parent fault/tip fault arrangement reported in Marchal et al. (1998) (see Fig. 2a). This isolated fault has probably been made by successive connections of tip faults to the growing parent fault. The indications of the composite nature of the principal fault termination are represented by relict connection zones. These former connection zones are manifested at the undulation points by a breached relay ramp (probably an earlier connection zone between the fault parts) and by an inactive branch of a linked secondary fault.

3.2.2. Overlapping and relay faults

The second set of traces studied forms a breached relay ramp. The relay zone is composed of two principal linked overlapping fault traces: the footwall fault trace (1; Fig. 4b) and the hanging wall fault trace (2; Fig. 4b). The two principal fault traces are connected by an oblique fault trace (3; Fig. 4b). Both principal fault traces have a high gradient of throw in the part of the termination involved in the relay zone formed with the oblique relay fault (4 and 5; Fig. 4b). Also noticeable is the secondary fault trace (4; Fig. 4b) extending from the principal trace of the footwall fault revealing a parent fault/tip fault type arrangement typical of the termination of an isolated fault as in Fig. 4a.

This set of fault traces shows the geometric relationship between two overlapping faults. This illustrates the connection of two isolated faults (1 and 2; Fig. 4b) by a relay fault (3; Fig. 4b), which could have resulted from the processes described in Fig. 2b. The sequence of these processes leads to the formation of a single composite, undulating trace. The secondary structures, which splay from the principal trace are the remains of intermediate connection stages.

The two above examples illustrate two normal fault configurations, which are commonly described from 2D data (e.g. Peacock and Sanderson, 1991, 1994; Wu and Bruhn, 1994). Nevertheless, such types of data do not resolve the spatial geometry of these structures. What are the relationships between the parent fault and the tip fault and between two overlapping faults at depth ? The answers to this question can be found by the 3D analysis of fault geometry.

4. 3D analysis of natural normal faults: morphology of fault planes from 3D seismic data

4.1. Normal faults in the Niger Delta

4.1.1. Geological setting

We examined a 3D seismic block from an oil field located in the onshore part of the Niger Delta. This field is bounded by a large N105-115°E striking growth fault (Fig. 5). The major faults are listric and connect at a decollement level, which is assumed to be at the top of the Akata Formation clays (Doust and Omatsola, 1990). The principal structure of this oil field is a collapsed rollover located in the hanging wall of the major growth fault F2 (Fig. 5). In the northern part of the structure, the rollover is bounded by the antithetic growth fault F1. This structure is affected by synthetic and antithetic minor faults. The minor faults are responsible for the division of the principal structure into small compartments (Fig. 5).

4.1.2. 3D geometry of the lateral termination

The 3D fault geometry of the studied seismic block can

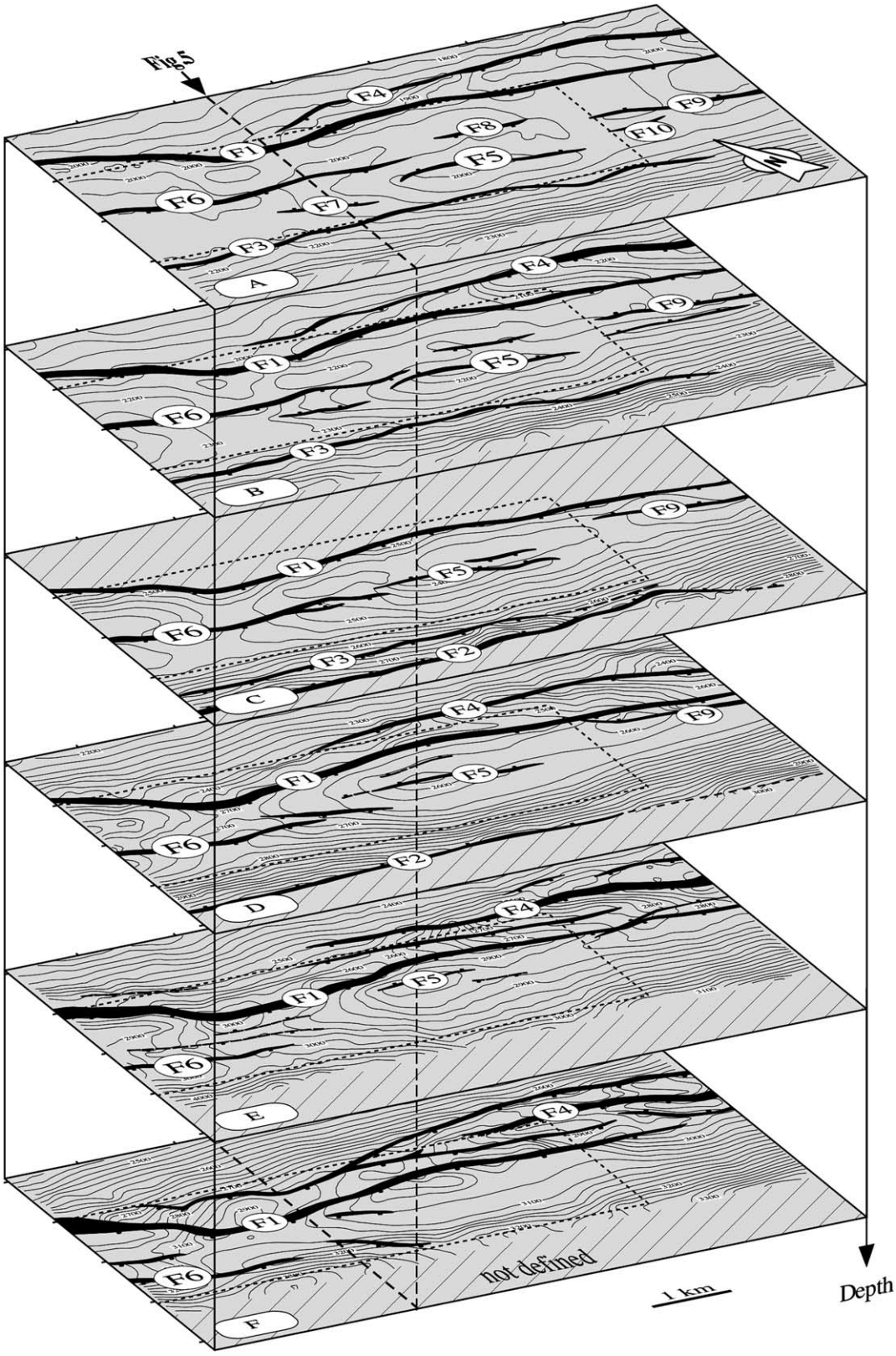

Fig. 6. 3D view of the fault network on structural maps at different depths (Niger Delta). Each map displays the fault trace network (heavy black) with the isobath contours of the chosen horizons (A to F; see Fig. 5). Detailed mapping shows that every single fault trace displays an undulating pattern along its entire length. The boxes (dashed lines) outline the views used in Fig. 7.

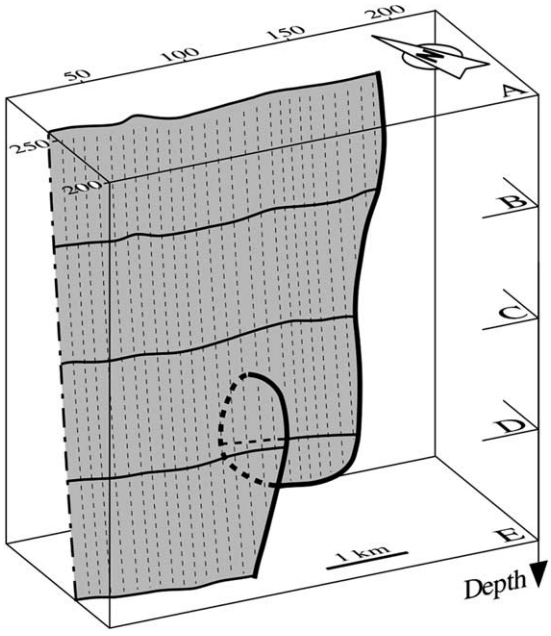

Fig. 7. 3D geometry of the lateral termination of normal fault F6. The heavy line shows the evolution of the tip line with depth and the horizontal lines are the footwall intersection of horizons with the fault plane. Thin vertical dashed lines are used to visualise the 3D geometry of the fault plane. The shape of the termination (see Fig. 6 for location) is characterised (i) by a zone of connection between a major fault plane and a secondary fault plane (horizons C and D) and (ii) a relay zone with F5 (see Fig. 6). The particular shape of this type of fault (bifurcation geometry) is due to disconnection of the secondary fault at depth. Vertical exaggeration ×6.

be seen from sections as well as from maps. However, the depth maps in the form of a block diagram (Fig. 6) give a more general view of the changing geometry of the fault traces at the different horizons. The traces of most faults display several undulations, which are found from one horizon to the next. Detailed examination reveals that the fault plane terminations have more undulations than the remainder of the fault plane. The termination traces are formed alternately of N95°E and N125°E segments (Fig. 6). This undulating pattern could be related to the propagation processes of an isolated normal fault (Marchal et al., 1998). Some large faults also extend into minor faults (e.g. the oblique trace at the tip of F6 on horizon D; Fig. 6). These minor faults are arranged in an en échelon pattern.

A close-up of the terminations of one such fault (F6) shows how fault trace geometry varies with depth (Fig. 7). Upwards, the fault traces are characterised by the following geometries:

1. Horizon E: the fault traces are simple and undulating;
2. Horizon D: the principal fault trace forms a relay zone with an en échelon secondary fault trace;
3. Horizon C: the two former fault traces are connected and form a longer undulating fault trace. A new point of inflection marks the former relay zone at this level.
4. Horizons B and A: the trace of F6 is longer than on the previous horizon but does not present a major change in its geometry (see Fig. 6).

The drawing of the lateral tip line of fault F6 shows a particular bifurcation caused by a connection zone between a parent-fault (principal plane) and a tip-fault (en échelon secondary fault plane). These types of bifurcations are also named ‘ear’ faults.

3D reconstruction of F6 fault shows that its plane is affected by two types of undulation (Fig. 8): (1) vertical undulation, which is characterised by a direction of its axis near the direction of the fault dip, and (2) horizontal undulation displaying a subhorizontal axis. As demonstrated above (see Fig. 9), the ultimate vertical undulation is the consequence of tip-to-parent fault connection. This suggests that the other vertical undulations are the relics of such former connection zones. Thus, fault F6 propagates by addition of new segments (tip-faults) at the termination of the principal fault plane. This process creates vertical undulations along the entire fault plane. The similarity between the terminations of the other faults (see Fig. 8) and those of fault F6 suggests that the major undulations result from similar processes. Horizontal undulation detected on fault F6 between horizons C and D is observed along the entire fault plane (Fig. 8). This horizontal undulation corresponds to a zone displaying a rapid decrease in throw values (Fig. 9). If we consider horizon F, the F6 trace appears much longer than its trace at horizon E (Fig. 9). Moreover, at horizon E, a secondary en échelon fault plane extends from the F6 trace. This observation linked to the decreased throw between horizons D and E suggests that the lower part of F6 (horizon E and F) has propagated upwards to link up to the upper part of F6 (horizons A to D) in the area of minimum displacement (black arrow; Fig. 9). Thus, horizontal undulation is probably an evidence of a vertical connection of the two fault planes that were initially separated and propagated towards each other. Such a process, also named dip linkage, has already been described by Mansfield and Cartwright (1996). The major undulations of normal fault planes result from both horizontal and vertical propagation processes.

In summary, all the major undulations found on the normal fault planes observed at the oil field scale seemingly result from the successive connection of secondary segments (tip faults) at the termination of the principal (parent) fault and the obliqueness of the tip faults.

4.2. Normal faults in the Gulf of Gabes

4.2.1. Geological setting

The second seismic block we studied, illustrating the 3D normal fault geometries, comes from a 3D seismic survey of the Gulf of Gabes in the southern Mediterranean Sea (Fig. 10). The studied area is affected by numerous N150°E–N160°E-striking normal faults with NE and SW dip forming a series of horsts and grabens. On the deepest horizons (not

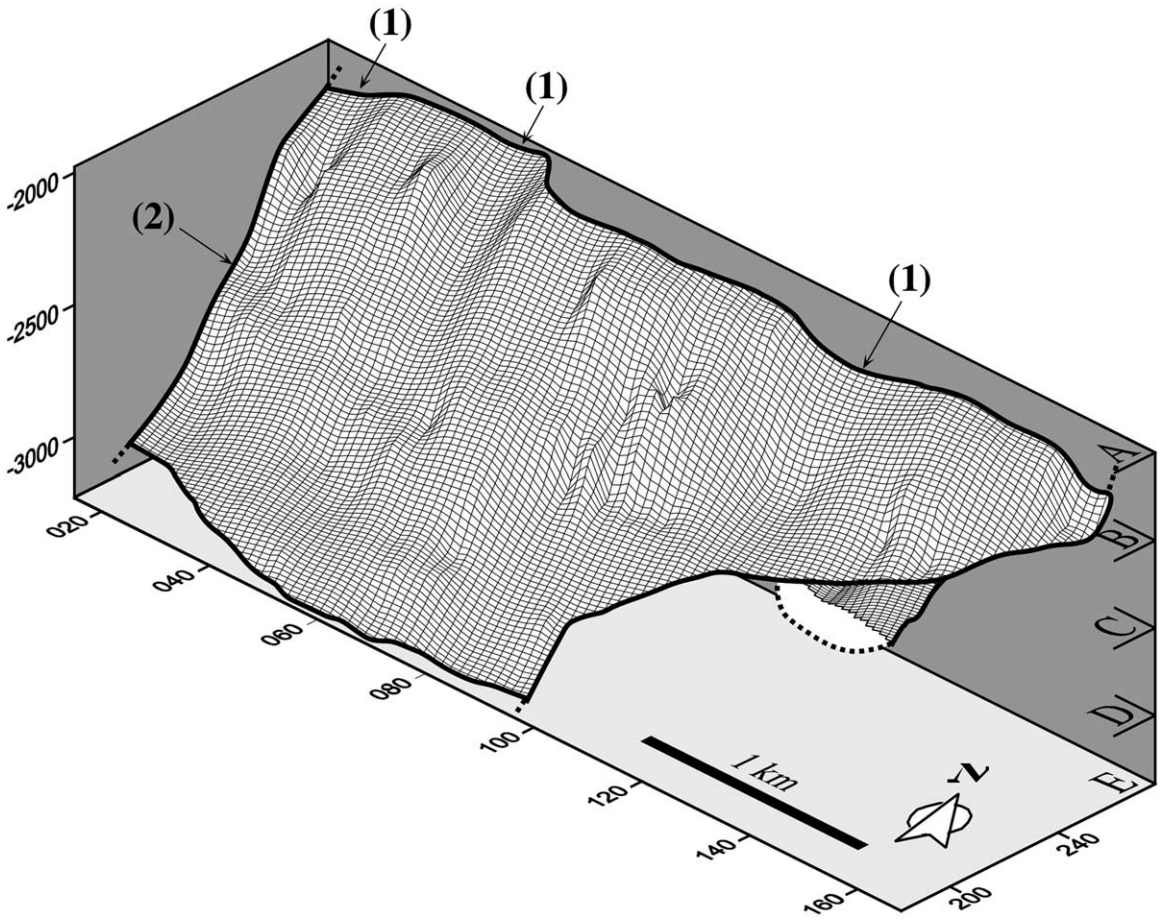

Fig. 8. Diagram illustrating the undulating morphology of a normal fault plane. This 3D view of F6 fault plane shows two types of undulating pattern: vertical undulation (1) and horizontal undulation (2). Both patterns are related to connection processes. Holes and bumps on the fault plane are artifacts. See text for details.

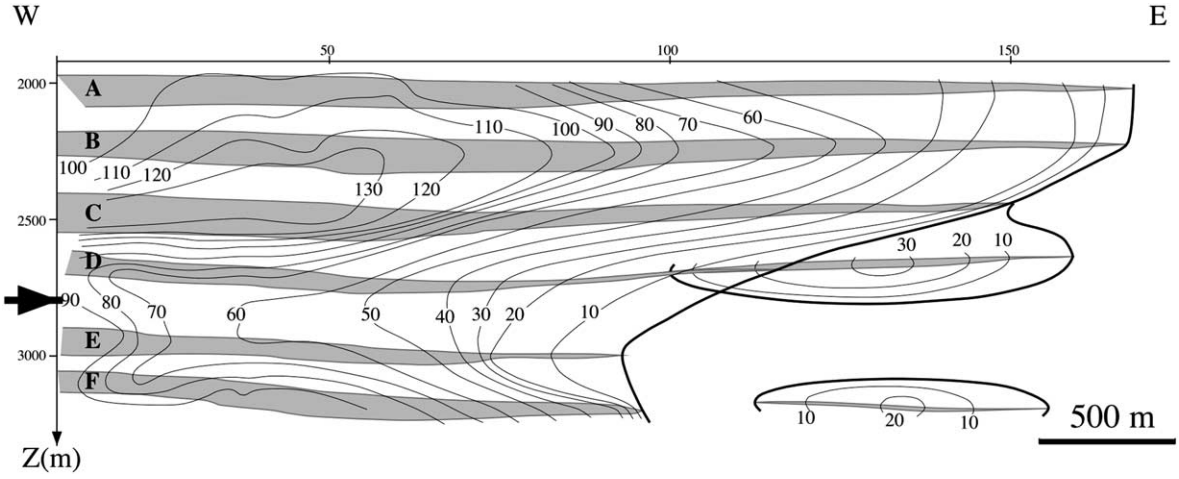

Fig. 9. Throw contour map of a complex normal fault plane. The map shows a throw strike projection of F6 in Fig. 6. The throw contours (in metres), represented by medium black lines, are derived from ca. 170 datapoints. The heavy lines show the tip line of the fault planes. The intersection lines (in grey) of the hanging wall and footwall parts of each mapped horizon (A to F) with the fault plane are shown and the offset zones are shaded. An area of substantial decrease in throw values (marked by a black arrow) can be seen between horizons D and E.

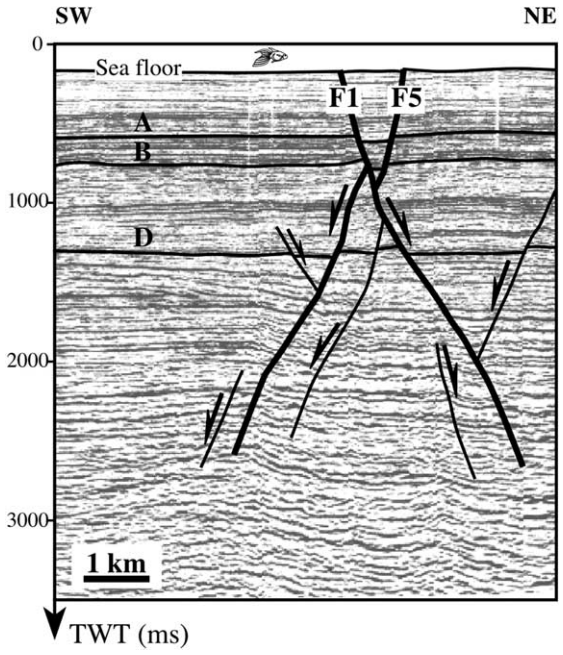

Fig. 10. Seismic section showing normal faults affecting the studied field (Gulf of Gabes). The line drawing emphasises the structural interpretation, i.e. the fault network and some of the horizons used to construct the structural maps in Fig. 11.

presented here) the major faults F1, F4 and F5 end in the same zone. This transition zone, where the major faults abut, is marked at depth by a N90°E–N100°E striking lineament cutting the basin into subunits. This lineament is interpreted to be a major fault affecting the Cretaceous basement.

In the upper part of the succession (tertiary and quaternary), the transition zone is not a fault but acts as a transfer zone of the extensional deformation between the northern and southern domains. This transfer zone is interpreted as an indirect expression of a deep N100°E striking structure (see Marchal, 1997). The influence of the deep fault diminishes rapidly with distance both vertically and horizontally. Thus, it is assumed that normal fault planes presented in this paper (F2 and F7; Fig. 11) are not influenced by the transfer zone.

4.2.2. 3D geometry of horizontal and vertical fault termination

The change in fault F2 geometry can be followed through many time maps of different horizons (Fig. 12). Generally the F2 traces lengthen from bottom to top (horizons F to A), with the increase in maximum throw values on the trace.

The traces of the fault zone present the following geometric pattern (Fig. 12):

1. From the deepest horizon (horizon F), F2 shows a comparatively limited trace and simple tips;
2. In the next two horizons up (horizons E and D) traces of secondary faults appear at the two terminations of F2. These faults form a relay arrangement with the termination of F2 and affect its footwall;
3. The transition to horizon C is characterised by connection of the secondary fault with the south-east end of the principal fault. The secondary fault trace located at the north-west tip of the main trace is still separate;
4. At the upper horizon (horizon B), the NW secondary fault traces are also connected to the principal plane trace;
5. At the last horizon surveyed (horizon A), the principal plane of the fault displays an undulating trace twice as long as in horizon F.

The geometry of the lateral terminations of this fault is much the same as that described above for the normal faults in the Niger Delta. The fault displays nearly symmetrical bifurcations ('ear' faults) at the lateral terminations, which are connected with the principal fault plane in their upper part. The bifurcations, which splay downward from the principal plane, indicate a downward propagating fault. Lower in the section, the bifurcations disappear. The direction of propagation is also indicated by the position of the bifurcation in relation to the connection zone with the major fault plane.

The F7 fault termination depicted on this 3D seismic survey also illustrates the segmented nature of a fault termination (Fig. 13). The fault trace was first drawn as a single fault plane (Fig. 13a). Detailed mapping of this termination reveals that in fact the fault zone consists of a set of small en échelon fault planes (Fig. 13b and c). Several relay ramps occur in the different overlap zones formed by the segment fault traces. These ramps seem to be breached at each extremity.

The lower traces of fault F7 illustrate the lower vertical termination of a normal fault (Fig. 14a). Childs et al. (1995) describe a very similar example of lower vertical termination (Fig. 14b).The lower vertical termination illustrated in Fig. 16a is marked by a set of en échelon secondary faults. In the upper part of the structure (horizon D; Fig. 14a), these tip faults are linked to the principal plane and tend to connect with each other upwards. Downwards from the principal plane, the planes of the tip fault rotate and become en échelon (horizon E; Fig. 14a). The 3D geometry of such a vertical termination is called lobate geometry.

5. 4D analysis of normal fault: evolution of the fault plane in space and time from 4D analogue modelling

The above 3D seismic examples show the present geometry of normal fault planes. But, how do faults reach this present geometry through time? Currently, the best way to study the evolution of faults in space and time is the analogue modelling imaged by X-ray tomography used in the 4D methodology (see Marchal, 1997; Marchal et al., 1998).

5.1. Experimental setting

We conducted a set of analogue models, using a two-layer

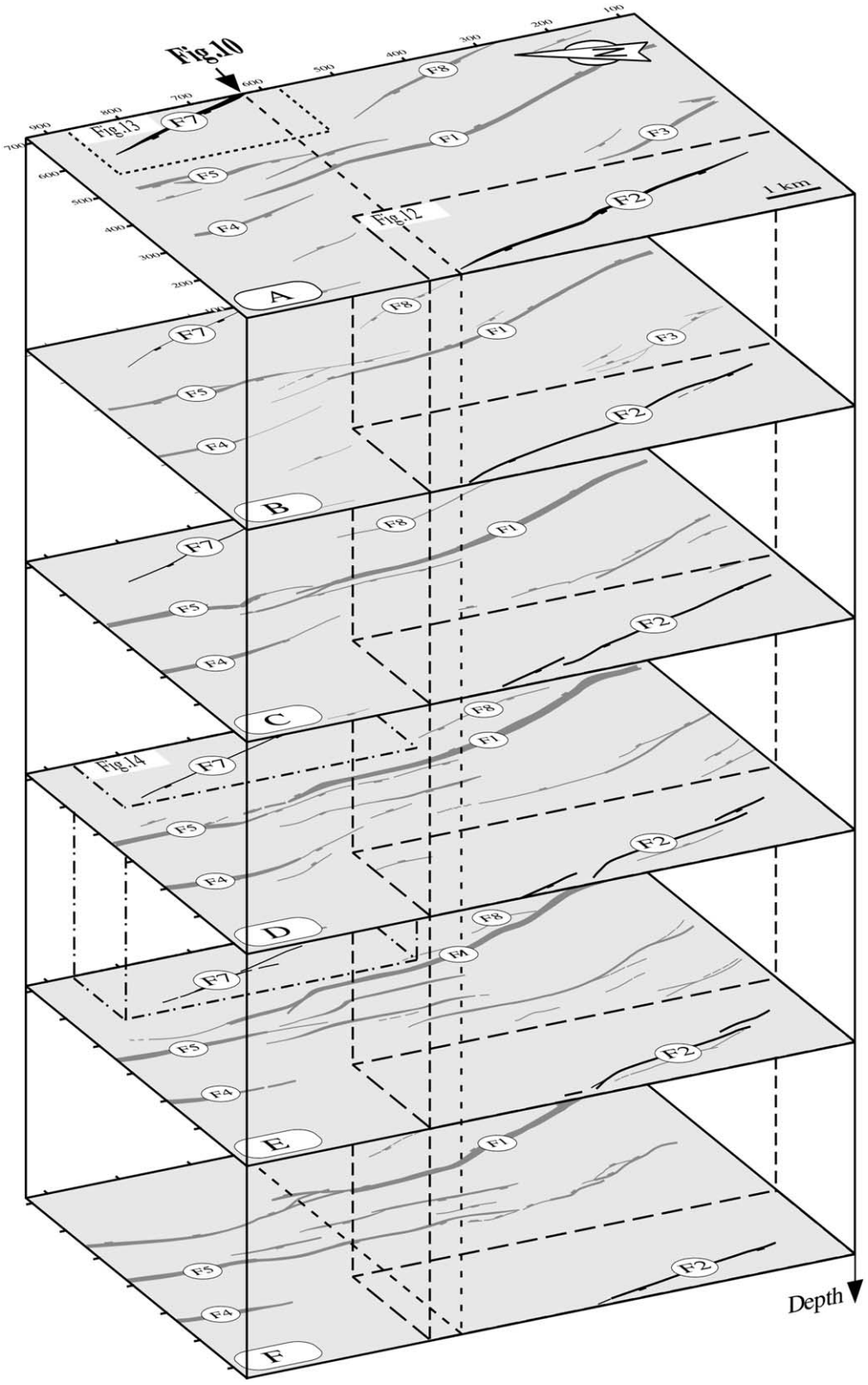

Fig. 11. 3D view of the fault network on structural time maps at different depths (Gulf of Gabes). Each map displays the fault trace network at the chosen horizon (A to F). The studied fault traces are shown as heavy black lines. The boxes outline the close-up views in Fig. 12 for F2 (dashed lines) and in Figs. 13 and 14 for F7 (chain lines).

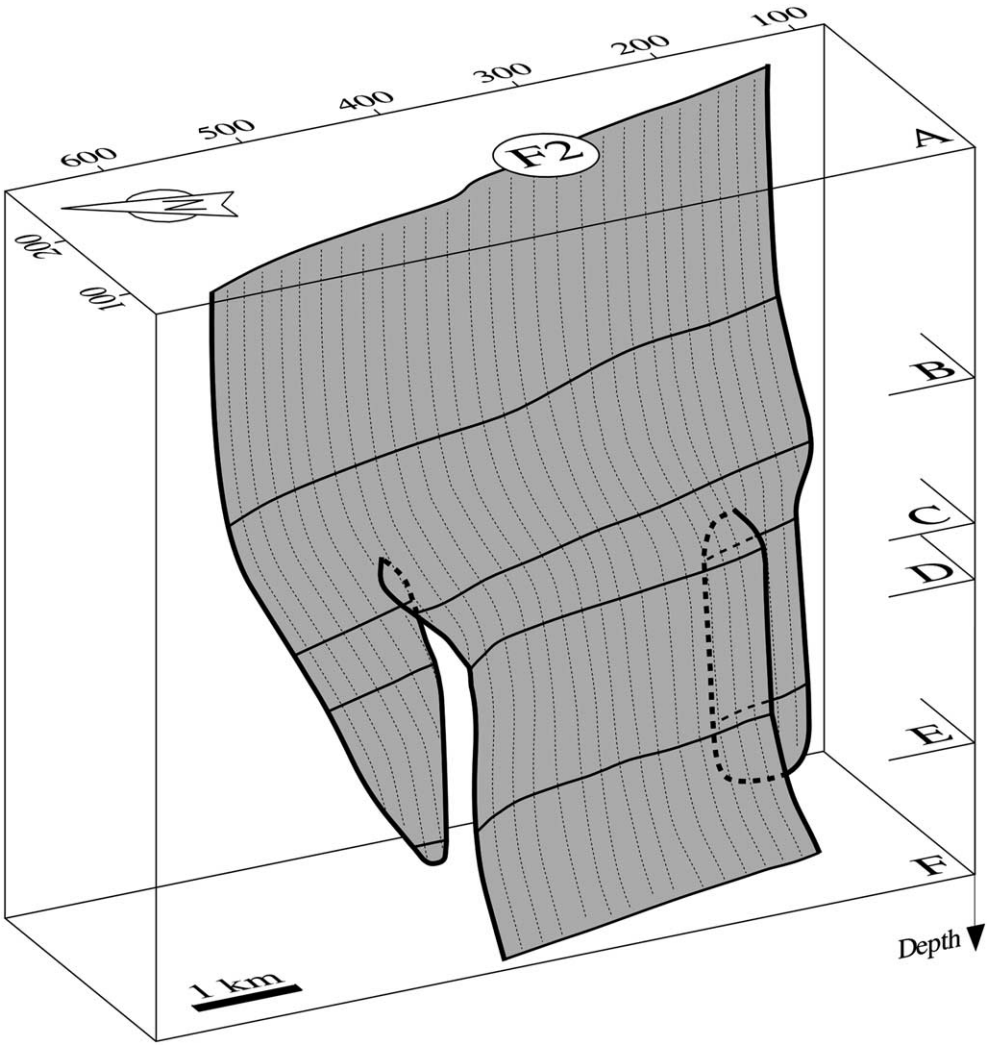

Fig. 12. Evolution with depth of the geometry of lateral terminations of normal fault F2 (see Fig. 11 for location). The heavy line shows how the tip line changes with depth and the horizontal lines are the footwall intersection of horizons with the fault plane. Thin vertical dashed lines are used to visualise the 3D geometry of the fault plane. The fault plane displays a typical bifurcation geometry at both lateral terminations of the fault zone. Connection zones between the parent fault plane and the tip fault planes are at approximately the same depth. Vertical exaggeration $\times 5$.

brittle–ductile design, similar to the works of Marchal et al. (1998). The models are composed of a thick basal viscous layer of silicon putty underlying a brittle layer composed alternately of sand and glass powder. Gravitational extension is initiated by a 1° slope at the base of the sandbox and controlled by a mobile wall, which allows the deformation to be halted at the principal steps. At each step, the 3D geometry of the fault network is studied through 3D picture block captured by X-ray tomography. The 3D block acquisition zone is centred on the middle of the model and its dimension calculated to avoid the zone of edge effects, which are anyway very limited.

We processed several analogue experiments to study the propagation processes and the geometry of normal faults. Here we present two representative examples of isolated normal faults to illustrate the horizontal and vertical evolution of fault plane geometry in space and time. The fault zones presented are from two separate 4D experiments (respectively, Figs. 15 and 16 and Figs.17 and 18).

5.2. Evolution of isolated fault terminations

After initiation, single isolated fault propagation is governed essentially by radial propagation and the tip-to-parent fault system.

5.2.1. Horizontal terminations

Isolated fault horizontal terminations display three typical geometries (Fig. 16), which are representative of the principal steps of propagation described above (see Fig. 2a):

1. In its initial configuration, the fault zone consists of one single main fault plane, which results from the processes of nucleation and initial propagation. This principal fault plane (parent fault) is approximately half-elliptical (fault

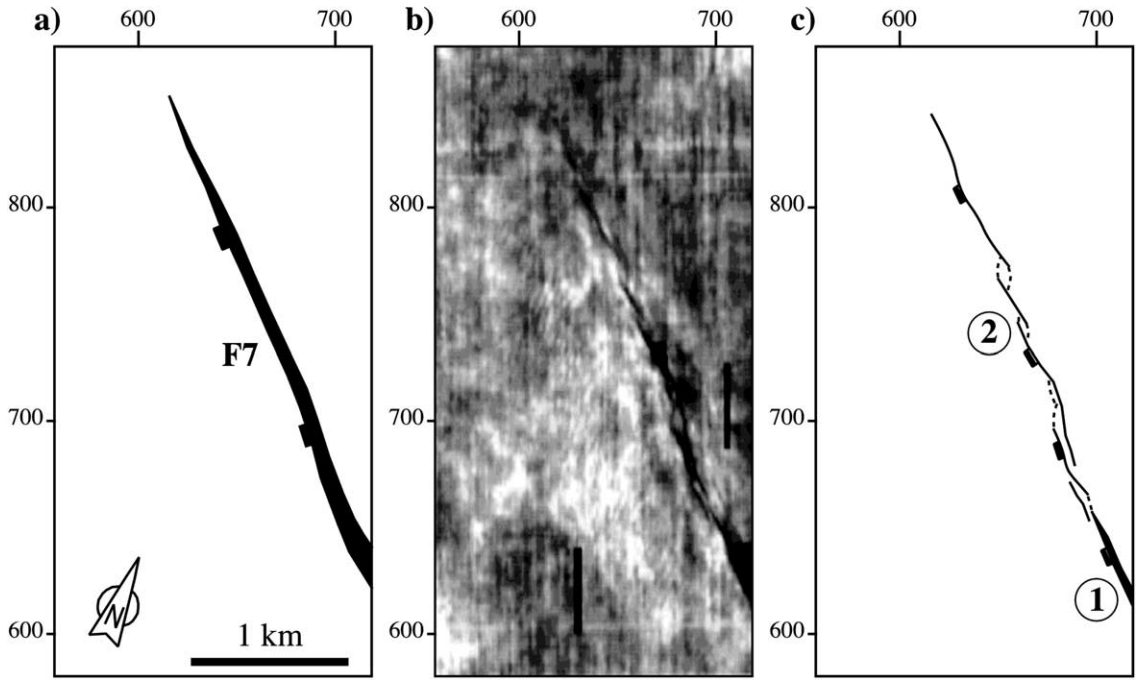

Fig. 13. Segmented horizontal termination of a normal fault. (a) Initial line drawing of the fault F7 lateral termination (horizon A; see Fig. 11 for location). (b) Detailed amplitude map of the fault termination. (c) Revised line drawing of the fault termination. Initially mapped as a single fault trace (see 1), the fault termination appears to be composed of a major fault plane termination (1) and a complex set of en échelon secondary faults (2).

initiated at the ductile–brittle interface and which propagates upwards) (F1; Fig. 16a);
2. In the intermediate configuration, a tip fault plane (F1a) appears at the lateral termination of the parent fault plane F1 (Fig. 16b), connected at its base to the latter. The resulting shape of the lateral termination is typical of upward bifurcation geometry (Fig. 16b). The tip fault and the parent fault form a relay zone breached by the footwall fault (FWBR; Fig. 16b). In our experiment, this type of relay zone displays arcuate fault terminations, which tend to propagate towards each other.
3. The third and final configuration displays a longer single but undulating and composite principal fault plane resulting from the total connection of the tip and parent fault planes (the two lower slices; Fig. 16c). The hanging wall part of the curved relay zone forms a relic of the former connexion zone (S.050; Fig. 16c). In our experiments, the final aggregated principal fault is rectangular because this plane, vertically, has reached the surface and, laterally, interacts with an other fault (see Section 5.3).

5.2.2. Vertical terminations

Vertical fault propagation, too, can be well imaged by analogue modelling with computerised tomography. The vertical propagation processes of isolated faults are better illustrated with single synthetic (or antithetic) fault systems, which display hanging-wall rotation (Fig. 17).

The upward propagation (i.e. vertical lengthening) of such faults occurs in three stages:
1. En échelon tip faults (secondary fault planes) develop along the vertical termination of the principal plane (slices 25; Fig. 18a to b) and are connected to the latter (slices 25–55; Fig. 18a, and slices 35–65; Fig. 18b);
2. The tip faults grow radially first and then overlap to form curved relay zones in the overlap zone (slice 25; Fig. 18a).
3. The tip faults inter-connect creating a new, longer, undulating principal fault plane with breached relay ramps (or/and horses) at the site of the former relay zones (slices 45; Fig. 18a to b).

This process may be stopped by soft or hard vertical linkage with another fault system or by a major interface (e.g. the free surface or a ductile layer).

The propagation process of isolated fault vertical terminations gives rise to a particular geometric configuration (Fig. 18), which is slightly different from those of horizontal geometry described above. Vertical terminations in the middle of a step of propagation are characterised by the en échelon bifurcations of the upper fault zone, which displays a typical lobate geometry. The undulations of the final fault zone are the result of the connection of the numerous tip planes (tip-to-tip process). The connection of certain parts of the tip fault planes in the relay zone tends to leave inactive secondary structures connected to the principal fault plane.

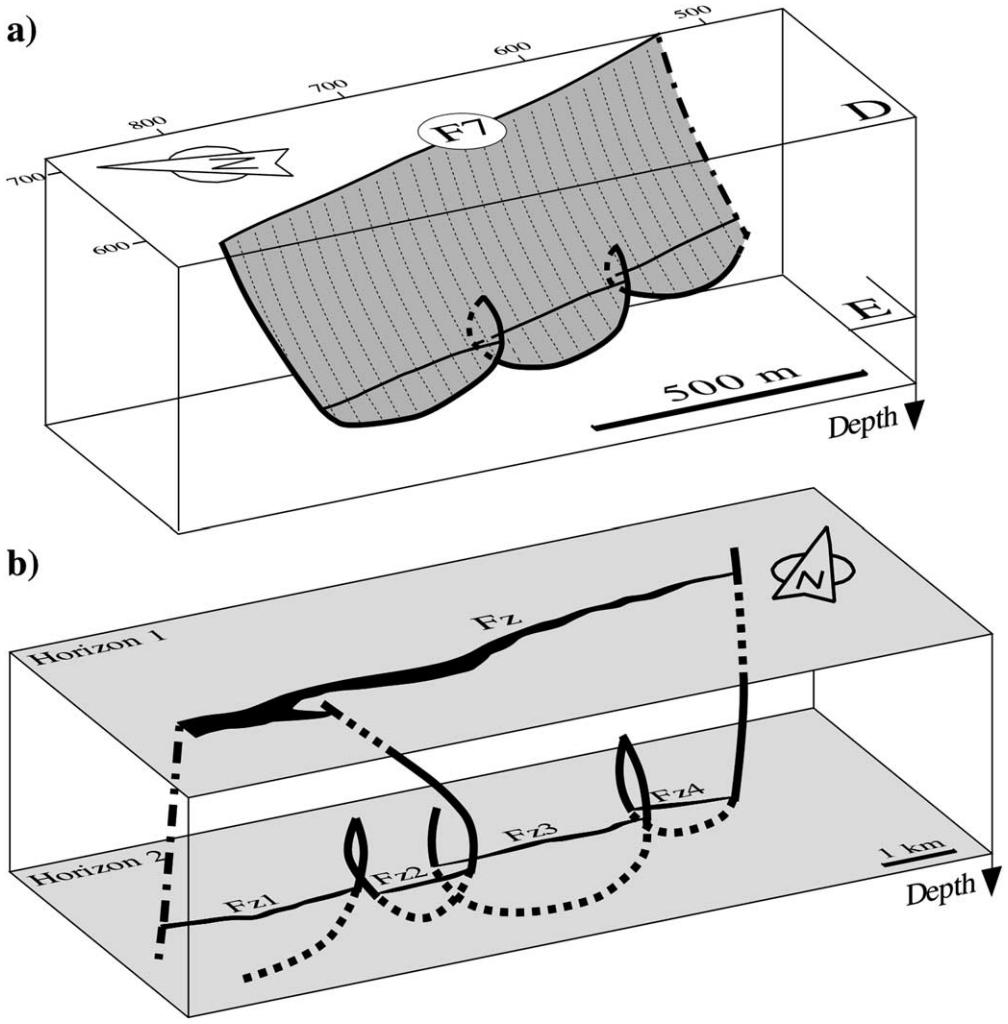

Fig. 14. 3D geometry of vertical terminations of normal faults. The heavy line represents the tip line of the fault. Thin vertical dashed lines are used to visualise the 3D geometry of the fault plane. (a) Vertical termination of F7 (see Fig. 11 for location). The fault plane displays a lobate geometry induced by the connection of en échelon secondary faults located at the front of the fault zone to the principal fault plane. (b) 3D view of vertical bifurcation (lobate) termination of a normal fault which probably propagated downwards (modified from Childs et al., 1995).

5.3. Evolution of isolated fault sets

Isolated fault set propagation occurs by interaction and linkage of single isolated faults in a relay arrangement. The resulting geometries corresponding to the different steps of linkage (see Fig. 2b) can be characterised by three types of geometry (Fig. 16):

1. The first type of geometry is achieved during the first step when the two isolated fault terminations display an overlap zone (not shown here). The two fault terminations form a single synthetic relay zone (cf. Morley et al., 1990 and in Fig. 16, step 4).
2. The second type of geometry arises when a relay fault appears in the relay zone (partially breached relay zone; Fig. 16b). The relay fault is globally half-elliptical and vertically elongated. The relay fault (F3) is connected to the hanging wall fault (F2) along its entire height, but to the footwall fault (F1) only at the lower level. The tip-line of the isolated fault termination is linear and vertical at the base of the displayed fault planes and curved towards the top (Fig. 16b).
3. The third distinctive geometry arises after the total connection of the relay fault with the two faults (completely breached relay zone; Fig. 16c). The single composite fault (F1F2F3) shows a large undulation in the place of the previous relay zone. Extending from the two inflection points composing the undulation, the two parts of the fault terminations in a relay arrangement with the relay fault display a straight vertical tip-line. Throw analysis show that these fault termination parts remain inactive by their connection with the relay fault (Marchal et al., 1998; Maerten et al., 1999).

The interaction between the two overlapping terminations should provoke an important decrease of fault propagation

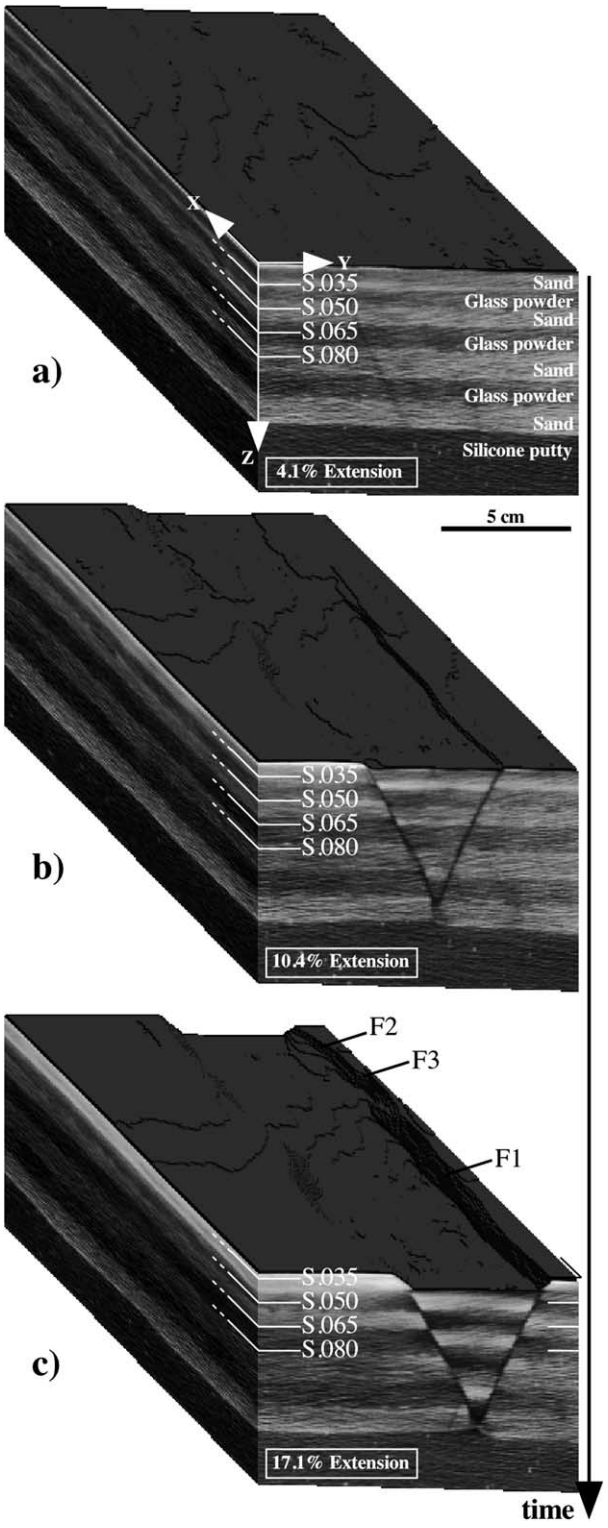

Fig. 15. 3D tomographic blocks, MODIFP2 experiment. These blocks show the different deformation steps (a to c) of the same model over time. Location of slices (S.035, S.050, S.065 and S.080) are shown in Fig. 16.

velocity (cf. Cartwright et al., 1995). The development of the relay fault should stop the lateral fault propagation. The two initially curved, interacting isolated fault tips tend to 'straighten' as they are deactivated by the connection of the relay fault to the two isolated fault terminations. These inactive parts of the isolated fault terminations in a relay arrangement with the relay fault form a large zone of deformation around the undulation zone.

Experiments suggest that the first order undulating pattern of normal faults results from the linkage process involved in isolated fault set propagation.

In summary, the 4D analogue modelling allows the visualisation of fault evolution in space and time and thus yields insights regarding the propagation processes. The geometrical results of the modelling are in good accordance with the geological data (2D, 3D). The 4D analysis gives useful interpretation guidelines to study the geometry and the kinematics of natural geological faults.

6. Geometric model of isolated normal fault planes

The shape of an isolated normal fault is not as simple as presented in some previous papers (Barnett et al., 1987; Walsh and Watterson, 1989; Mansfield and Cartwright, 1996; Nicol et al., 1996; Willemse et al., 1996). The different geometric features of normal fault planes are synthesised in a conceptual model (Fig. 19). Combining the different parts (i.e. terminations) of the studied normal fault planes, this geometrical model represents the idealised plane of an isolated normal fault.

6.1. Geometrical characteristics

The model is divided into four parts, each representing a specific configuration of normal faults (Fig. 19). Each part of the model displays a lateral and a vertical termination. The lateral terminations are marked by oriented (downward or upward) bifurcations. Two bifurcation geometries can occur at the lateral termination, depending on the sense of propagation: the upward and the downward bifurcation geometry. These oriented bifurcation geometries are made up of linked secondary en échelon fault planes. The vertical terminations display a particular configuration called 'lobate' geometry. Lobate bifurcations are induced by the growth of small en échelon fault parts at the propagating vertical termination. Both lateral and vertical bifurcation geometries correspond to the development of secondary fault planes (tip faults) at the principal fault plane (parent fault) terminations. Tip fault orientations are slightly different from the principal plane orientation. The perturbed stress field occurring at the fault terminations (i.e. Petit and Barquins, 1993; Willemse, 1997; Crider and Pollard, 1998) implies these differences of fault plane orientation at the origin of the particular termination geometries.

Our model can be used to describe most normal faults (Fig. 19):

1. The geometry of normal faults subjected to downward propagation is represented by the two lower blocks;
2. The geometry of normal faults subjected to upward

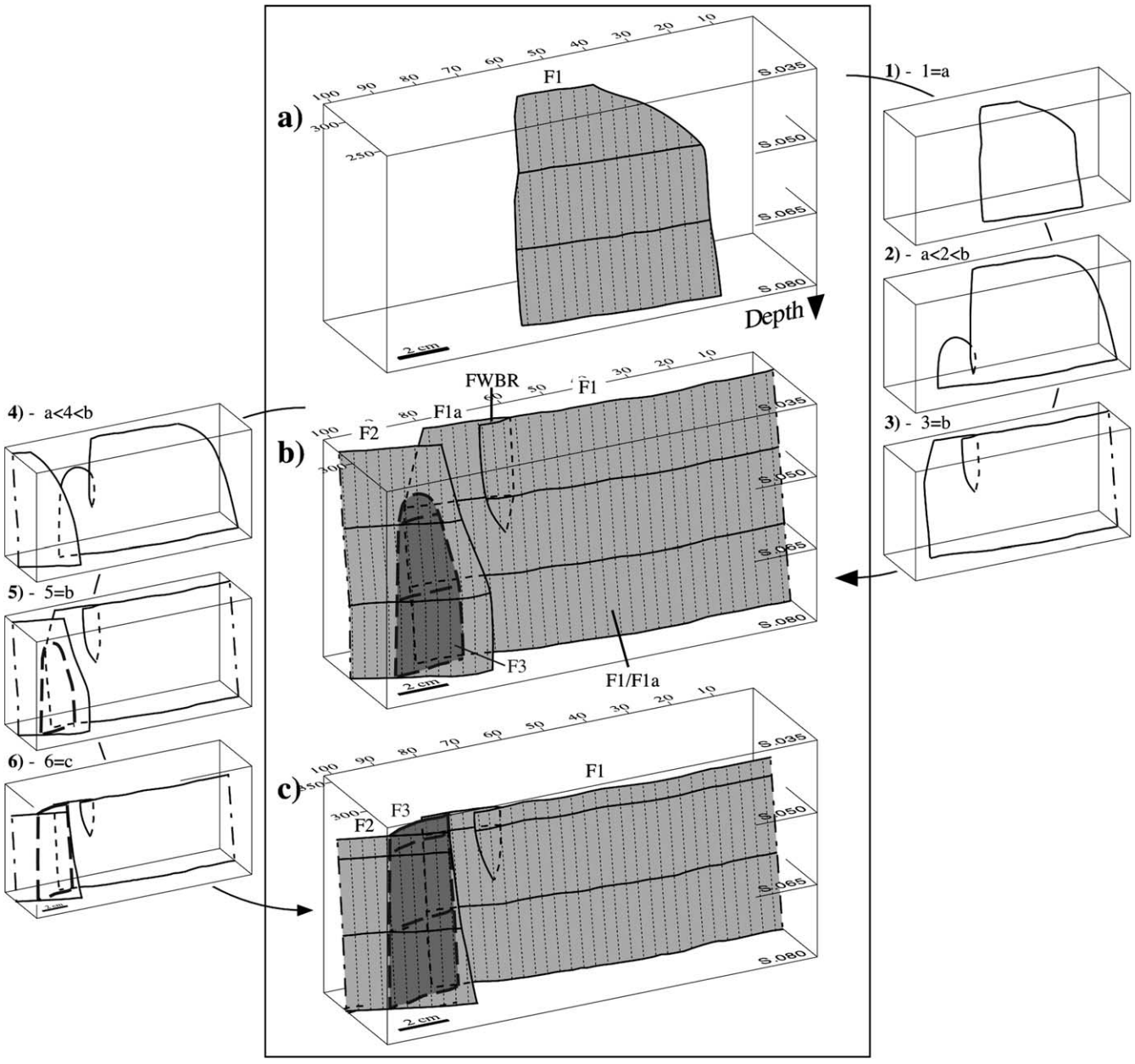

Fig. 16. 4D development of isolated normal faults. The three diagrams (a to c) show the lateral geometric evolution of fault planes developed in an analogue model over time. FWBR = footwall breached relay zone *sensu* Trudgill and Cartwright (1994). (1 to 3) The three characteristic geometries associated with isolated fault propagation. (1) Single parent fault plane. (2) Lateral bifurcation geometry: parent fault plane with a tip fault plane developing at its termination. (3) Connected lateral bifurcation geometry. Note that (2) is inferred from (1) and (3). (4 to 6) The three typical geometries associated with overlapping fault propagation. (4) Single synthetic relay zone. (5) Relay zone partially breached by a relay fault. (6) Relay zone completely breached by a relay fault. Note that (4) is infered from (5). See text for details. Experiment MODIFP2.

propagation is represented by the two upper blocks;

3. The geometry of normal faults subjected to both downward and upward propagation is represented by all four blocks.

Composite normal faults can be also represented. For example, the geometry of a normal fault composed of two parts propagating towards each other can be illustrated by inverting the two lower blocks with the two upper blocks of the model (see Fig. 9). The idealised fault plane shown in Fig. 19 displays a circular fault shape (aspect ratio = 1) (see Nicol et al., 1996; Willemse et al., 1996). The four blocks of the model can be moved horizontally and vertically to accommodate the different fault shapes: tall faults (aspect ratio < 1) and elongated faults (aspect ratio > 1).

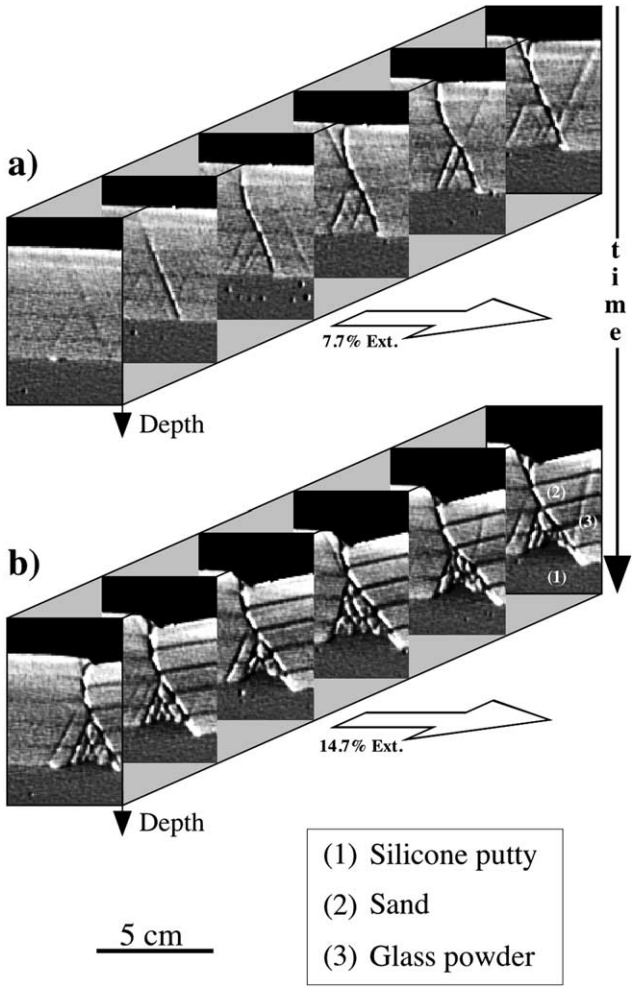

Fig. 17. 3D tomographic blocks, MODIFP4 experiment. These blocks are represented by equidistant vertical sections and show two strategic deformation steps (a to b) of the same model over time. The 3D blocks are used to create the slices displayed in Fig. 18.

6.2. 2D view of the 3D model: fault traces

Horizontal and vertical 2D slices can be made from the 3D geometric model (Fig. 19). Depending on the position of the horizontal slice on the fault zone, the geometry of the fault traces on the displayed vertical slices are quite different. The length and orientation of the segments composing the horizontal fault trace may vary as well as their number. Such variations are also possible with vertical fault traces. With knowledge of the 3D structure of the fault zone, the analysis of 2D slices can give some information about the structural position of these slices with regard to the general fault structure.

6.3. Nomenclature

In the proposed model, normal faults propagate essentially by connection or branching processes, particularly at the fault terminations. One of the major features resulting from this type of propagation is the relay zone, which is built up of two overlapping fault segments. Because offsets between two fault segments can occur in any direction (Aydin and Nur, 1985; Peacock and Sanderson, 1994; Childs et al., 1996b), Peacock and Sanderson (1991) give a general geometrical definition for offsets applicable to all fault classes. Offsets (or overlap in Childs et al., 1995, 1996a) can be divided into 'displacement-parallel offsets' and 'displacement-normal offsets' (respectively, in-plane oversteps and anti-plane oversteps for Peacock and Zhang (1994)) which are, respectively, offsets in plan view and offsets in cross-section for a dip-slip fault (Fig. 20a). Both preceding types of offsets can be subdivided into those which are contractional (or restraining) and extensional (or releasing) (Peacock and Sanderson, 1991; Childs et al., 1996a). But, in the case of a normal fault, contractional and extensional offsets are only applicable to displacement-parallel offsets. For displacement-perpendicular offsets, it would be preferable to distinguish right-stepping offsets and left-stepping offsets as in en échelon segment nomenclature (Fig. 20a).

At a more mature stage, an overlap relay zone generally evolves into an undulation (Fig. 20b). One type of offset corresponds to one type of undulation. Thus, undulation nomenclature should follow offset nomenclature. Here, we distinguish displacement-parallel to displacement-perpendicular undulations corresponding, respectively, to horizontal and vertical undulations for a normal fault. These two types of undulation can also be divided into restraining and releasing undulations for displacement-parallel undulation types and into right-stepping and left-stepping undulations for displacement-perpendicular undulation types (Fig. 20b).

These two geometrical classifications (overlap relay zones and undulations) provide all the tools for describing the 3D geometry of isolated normal faults.

6.4. Evolution of normal fault geometries

6.4.1. Evolution of isolated normal faults

Three principal processes should occur in isolated normal fault propagation: radial, tip-to-parent fault and tip-to-tip fault propagation. In this study, radial propagation is involved for processes below the resolution of the acquisition system used. Thus, the fault seems to propagate in its own plane. At a given stage of deformation, tip faults develop around the entire border of the principal plane (Fig. 21a). Fault growth is characterised for both horizontal and vertical terminations. The tip-to-parent fault process is responsible for the lateral bifurcation geometry occurring at the horizontal terminations of the isolated fault. In this process, the tip fault connects with the parent fault by way of a curved relay zone to form a new principal fault plane part. Vertical termination is governed by tip-to-tip fault propagation, which is at the origin of the lobate geometry displayed by the upper and the lower terminations of the isolated fault. In this process, the tip faults connect up by way of relay zones. Already linked to the parent fault plane,

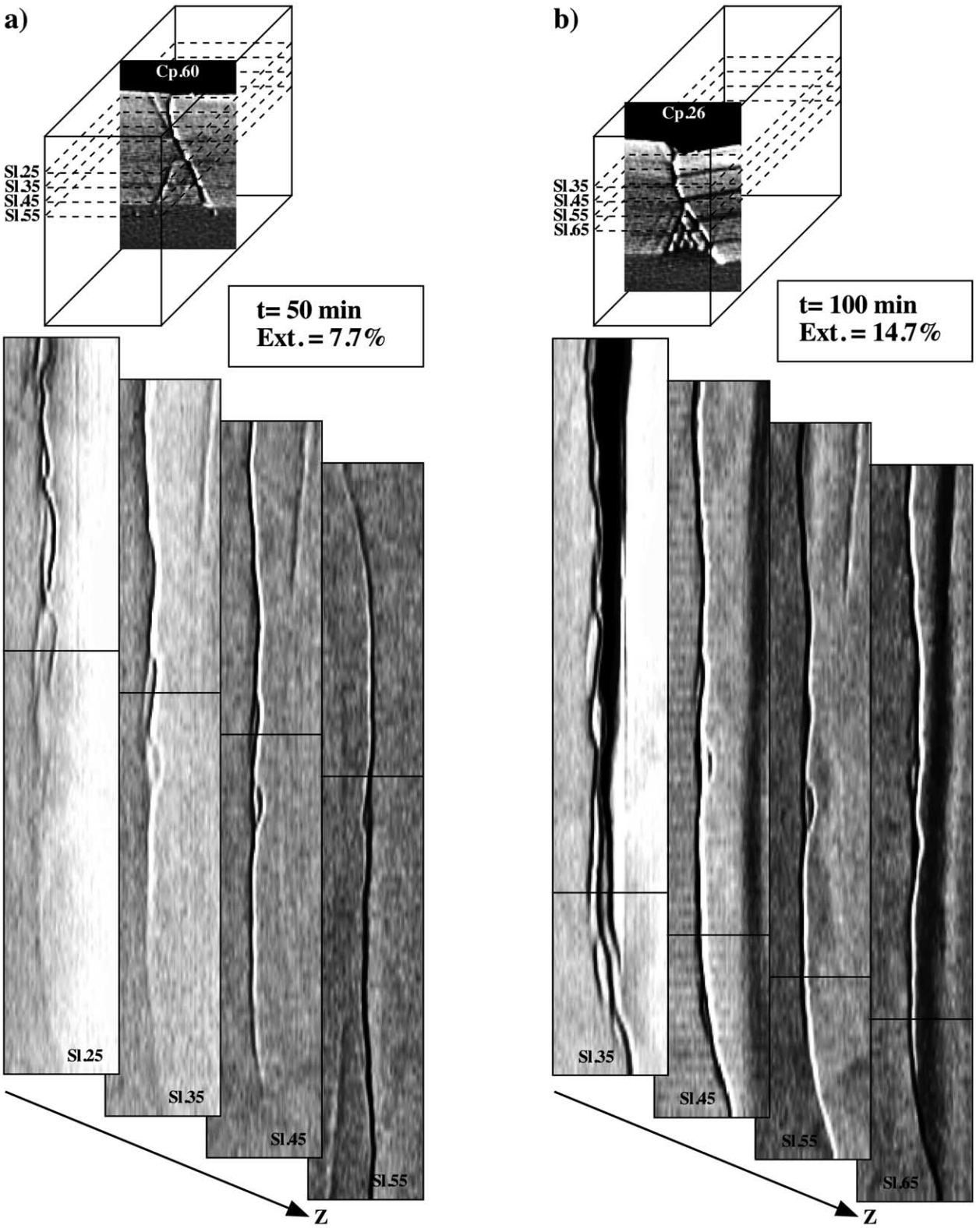

Fig. 18. 4D vertical evolution of isolated normal faults. The two sets (a and b) of horizontal slices show the upward geometric evolution of fault planes developed in an analogue model over time. See text for details. Experiment MODIFP4.

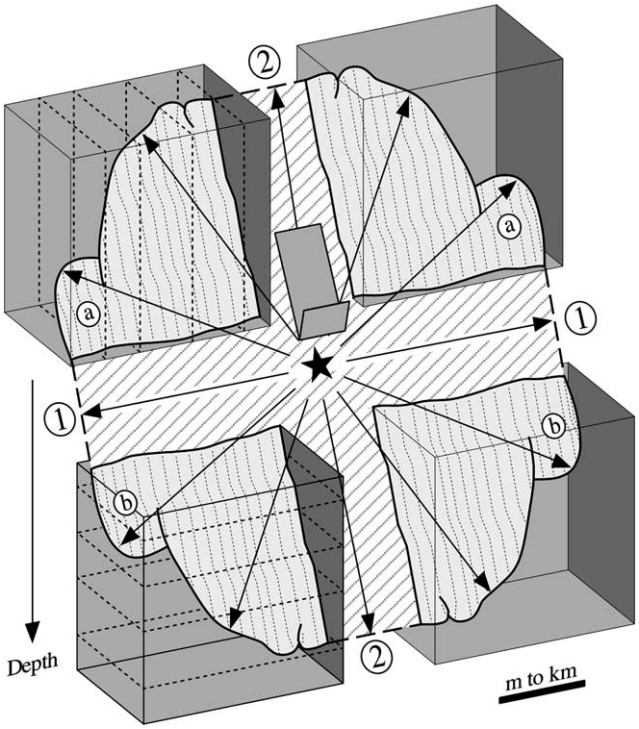

Fig. 19. 3D conceptual model of an isolated normal fault. Each of the four boxes contain a quarter of the normal fault plane. The terminations display the lateral (1) and vertical (2) bifurcation geometries. The lateral bifurcation geometry is divided into upward (a) and downward (b) configurations. Both lateral and vertical (lobate) bifurcation geometries are represented in two basic configurations: for an upward propagating fault (the two upper boxes) and for a downward propagating fault (the two lower boxes). The 3D geometry of a normal fault which propagates 'radially' (i.e. downwards and upwards) is represented by the plane defined by the four boxes. The star marks the initiation zone of the fault. The thin arrows indicate the propagation directions and the large arrow shows the sense of slip. The heavy dashed vertical and horizontal lines show the position of cross-sections and horizontal slices across the 3D structure. Thin vertical dashed lines are used to visualise the 3D geometry of the fault plane. See text for details.

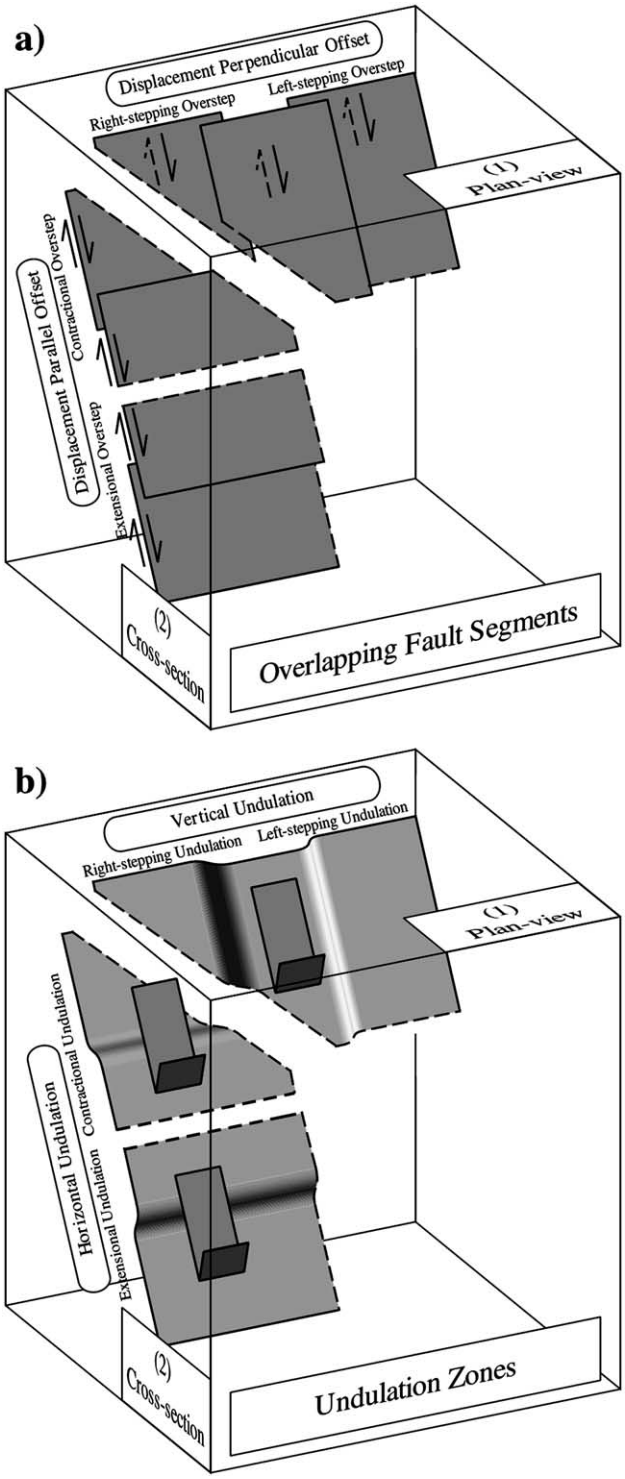

Fig. 20. Nomenclature of the normal fault plane relationships. (a) Diagram showing the horizontal (1, plan view) and vertical (2, cross-section) relationships between overlapping normal fault segments 'before connection'. (b) Diagram showing the horizontal (1, plan view) and vertical (2, cross-section) nomenclatures of undulation zones derived from the overlapping normal fault segments.

the linkage of the tip faults creates a new principal fault plane part. We suggest that the propagation process occurring at the border of the isolated fault between the horizontal and the vertical terminations is a combination of both tip-to-parent and tip-to-tip fault linkage process (Fig. 21a). The two above linkage processes still occur as long as the isolated fault terminations (horizontal or vertical) remain isolated, i.e. no soft or hard linkage with another isolated fault system.

6.4.2. Evolution of isolated normal fault set

The evolution of the geometry of isolated fault sets is governed by the isolated-to-isolated fault propagation process (Fig. 21b). The horizontal connection between two isolated faults occurs in three steps. First, the tip-to-parent propagation of each isolated fault termination is locked by interaction between the two overlapping faults in the relay zone. Secondly, an oblique relay fault is initiated in the relay zone, generally at the top of the ramp. Thirdly,

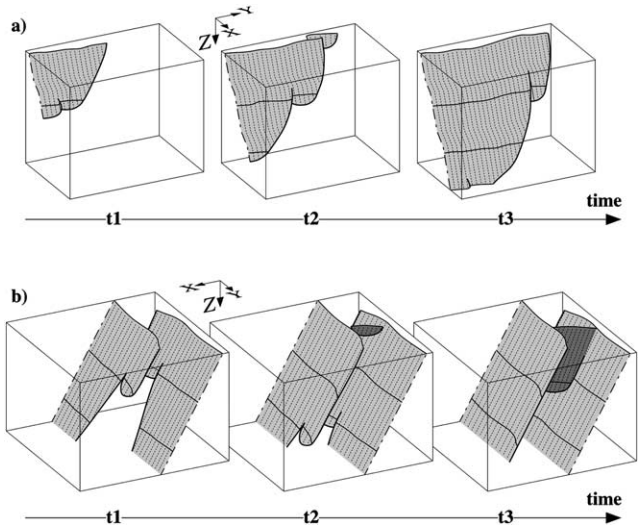

Fig. 21. 3D conceptual models of geometrical evolution of normal faults. (a) 4D sequence of the right-lower quarter of an isolated fault showing the evolution of both horizontal and vertical terminations. The geometry of the horizontal and vertical terminations is governed, respectively, by tip-to-parent and tip-to-tip fault linkages, which occur until the termination remains isolated. (b) 4D sequence of two overlapping fault terminations. The geometry of the fault planes is governed by isolated-to-isolated fault linkage. See text for details.

the relay fault connects up the two terminations. Once the isolated fault is totally connected by the relay fault, the deformation is accumulated on a single, but composite and undulating, fault plane. During linkage, the terminations of the isolated faults overlapping the relay fault become progressively inactive. An equivalent process probably occurs for vertical connection between two isolated faults.

7. Discussion

Detailed information and precise conceptions about normal fault geometry and morphology are of great importance in petroleum geology. The detailed study of fault propagation yields valuable information about fault plane 'heterogeneities' and the geometry of their terminations, which is essential for defining, for example, the accumulations or working volumes, respectively, in the case of hydrocarbon production or storage.

7.1. Tip faults and bifurcations

In our model, we suggest that principal normal fault planes propagate by way of secondary minor fault planes (tip faults) initiated at the termination of the principal fault plane. Secondary structures are not always shown at the terminations of the major fault planes. The major reason for the scarcity of good pictures of natural lateral and vertical bifurcation terminations is that such small structures can be principally studied in 3D. Detailed study of the geometry of terminations reveals the presence of segmented secondary structures such as tip faults (see Fig. 13). The 2D analysis of vertical terminations has led to misinterpretation of 3D geometry (Walsh and Watterson, 1991; McGrath and Davison, 1995). In the studies of these previously cited authors, the tip faults are not connected parallel. Nevertheless, 3D analysis shows that these tip-faults (bifurcations) are connected to the principal plane and arranged in an en échelon pattern.

No natural upper vertical termination such as presented by the geometrical model has been well expressed in our study and only a few geological examples of such structures are described in the literature (Larsen, 1988; Childs et al., 1995; Rawnsley et al., 1998). Nevertheless, upper segmented vertical terminations are perhaps not so rare as we may think. Normal fault vertical terminations are currently studied principally in cross-section (e.g. Peacock and Zhang, 1994; Childs et al., 1996a), which does not favour observation of these inherently 3D structures. Three-dimensional views of such natural structures can be accessed only by exceptional exposure conditions. For example, Rawnsley et al. (1998) show in their figure 5 a natural structure which may be interpreted this way.

7.2. Mechanical and rheological controls of normal fault termination segmentation

The study of normal fault 3D geometry reveals the irregularities of fault plane borders. Segmentation occurs at both lateral and vertical terminations. Tip fault development clearly increases the segmentation at the fault terminations at a given stage of propagation. As shown by the natural examples presented and analogue modelling, secondary fault planes are invariably displayed as being connected to the principal fault planes. We suggest that the tip faults are initiated at the termination of the parent fault and grow away from the principal plane. Thus, tip faults are always connected to the parent (principal) fault plane in opposition to the geometrical model proposed by McGrath and Davison (1995) (see 3; Fig. 1b). This assumption is emphasised by the results of mechanical studies of crack and fracture propagation (Pollard et al., 1982; Petit and Barquins, 1988; Cooke and Pollard, 1996). These types of study have also shown that the general stress field is highly disturbed around the fault termination (i.e. Petit and Barquins, 1993). This disturbed stress field may cause variations in tip fault plane orientations with regard to the principal fault plane direction. This phenomenon leads to the segmentation of normal fault terminations.

In earlier work (Peacock and Zhang, 1994; Childs et al., 1996b), strong rheological interfaces in the sedimentary cover are invoked to explain segmentation at normal fault terminations. We believed that, if rheological interfaces can be responsible for vertical segmentation, they cannot be involved in lateral segmentation processes. Both lateral and vertical bifurcations correspond to the development of secondary fault planes (tip faults) at the principal fault plane (parent fault) terminations (see Fig. 19) but they lead to

different geometries by reason of their positions on the principal fault plane with regard to the stress field (see Kattenhorn et al., 2000). The vertical bifurcations occur at the termination of the fault, which is dominated by the mode II fracture mechanics while the lateral configurations occur in a zone subjected to the mode III fracture mechanics. Both mode II and III fracture mechanics lead to out-of-plane propagation but, while mode III configuration implies clearly the propagation of segmented structures in various homogenous media (e.g. Petit and Barquins, 1993; Cooke and Pollard, 1996), the deformation generated by mode II configuration shows various types of out-of-plane fractures (e.g. Petit and Barquins, 1988; Cooke and Pollard, 1996). However, Marchal (1997) noticed the large predominance of mixed mode II + III configurations occuring at the normal fault terminations, which produce out-of-plane segmented fractures. In this paper, we assume that the segmentation of the terminations is genetically induced by the propagation process but, considering the data presented by Peacock and Zhang (1994) and Childs et al. (1996b), are currently enhanced by a lithological and rheological contrast between the sedimentary layers.

8. Conclusions

Detailed analysis of 3D fault plane geometry shows the complex nature of normal fault zones:

1. Geometry of normal faults is governed by four types of propagation process: (i) radial propagation, (ii) tip-to-tip fault connection, (iii) tip-to-parent fault connection, and (iv) isolated-to-isolated fault linkage.
2. Normal faults display characteristic geometries at their terminations: oriented lateral bifurcation geometry and lobate geometry.
3. Both lateral and vertical bifurcation geometries result from propagation processes consisting in the growth of secondary fault planes from the termination of the principal plane of the fault zone.
4. Both lateral and vertical terminations of a normal fault plane may be segmented and therefore amenable to the formation of fluid leak points.
5. Secondary fault planes are arranged in an en échelon pattern and form a relay zone with the principal plane for horizontal terminations and together for vertical terminations of the fault zone.
6. As deformation evolves, displacement occurs on one single composite fault plane, which becomes the new principal fault plane. New tip faults develop from this new principal plane if the terminations remains 'isolated'.
7. Inactivated secondary structures are currently observed branched to the principal plane (either in the hanging wall or in the footwall) and located at the inflection point of the principal plane undulations.
8. The geometrical variability of fault traces is representative of different 2D views of a single complex 3D geometry.
9. With our model, complex geometry can be depicted in relation to the horizontal and vertical propagation history of the composite fault plane.

Our model offers a general view of normal fault plane geometry and accounts for most geometric characteristics of normal faults. This is made possible by an approach combining the analysis of data from different origins and of different types. Although detailed geometry of a naturally-occurring normal fault is probably more complex than the model shows, mainly because of local parameters, our model provides a good basis for observing and analysing the 3D geometry of normal faults in many cases.

Acknowledgements

The work reported forms part of the Ph.D. research of D. Marchal who would like to thank Elf Exploration-Production for funding. We are also grateful to Elf Exploration-Production for providing the 3D seismic datasets and for permission to publish this paper. We are indebted to B. Colletta and J.M. Mengus for their invaluable assistance in conducting the experiments and for the use of the X-ray tomograph of the Institut Français du Pétrole. We thank also B. Colletta, J.M. Daniel and J. Letouzey for useful discussions that considerably improved the manuscript. We would also like to express our gratitude to the J. Cartwright, L. Maerten and J.P. Evans for their constructive reviews and helpful suggestions.

References

Antonellini, M., Aydin, A., 1995. Effect of faulting on fluid flow in porous sandstones: geometry and spatial distribution. American Association of Petroleum Geologists Bulletin 79, 642–671.

Aydin, A., Nur, A., 1985. The types and role of stepovers in strike-slip tectonics. In: Biddle, K.T., Christie-Blick, N. (Eds.), Strike-slip Deformation, Basin Formation, and Sedimentation. Special Publications of the Society of Economics Palaeontology and Mineralogie 37, pp. 35–44.

Barnett, J.A.M., Mortimer, J., Rippon, J.H., Walsh, J.J., Watterson, J., 1987. Displacement geometry in the volume containing a single normal fault. American Association of Petroleum Geologists Bulletin 71, 925–937.

Bruhn, R.L., Schultz, R.A., 1996. Geometry and slip distribution in normal fault systems: implication for mechanics and fault-related hazards. Journal of Geophysical Research 101, 3401–3412.

Cartwright, J.A., Mansfield, C.S., 1998. Lateral displacement variation and lateral tip geometry of normal faults in the Canyonlands National Park, Utah. Journal of Structural Geology 20, 3–19.

Cartwright, J.A., Trudgill, B.D., Mansfield, C.S., 1995. Fault growth by segment linkage: an explanation for scatter in maximum displacement and trace length data from the Canyonlands Grabens of SE Utah. Journal of Structural Geology 17, 1319–1326.

Childs, C., Watterson, J., Walsh, J.J., 1995. Fault overlap zones within

developing normal fault systems. Journal of the Geological Society of London 152, 535–549.

Childs, C., Nicol, A., Walsh, J.J., Watterson, J., 1996a. Growth of vertically segmented normal faults. Journal of Structural Geology 18, 1389–1397.

Childs, C., Watterson, J., Walsh, J.J., 1996b. A model for the structure and development of fault zones. Journal of the Geological Society of London 153, 337–340.

Cooke, M.L., Pollard, D.D., 1996. Fracture propagation paths under mixed mode loading within rectangular blocks of polymethyl methacrylate. Journal of Geophysical Research 101, 3387–3400.

Cowie, P.A., Scholz, C.H., 1992. Physical explanation for the displacement–length relationship of faults using a post-yield fracture mechanics model. Journal of Structural Geology 14, 1133–1148.

Cowie, P.A., Shipton, Z.K., 1998. Fault tip displacement gradients and process zone dimensions. Journal of Structural Geology 20, 983–997.

Crider, J.G., Pollard, D.D., 1998. Fault linkage: three-dimensional mechanical interaction between echelon normal faults. Journal of Geophysical Research 103, 24373–24391.

De Polo, C.M., Clark, D.G., Slemmons, D.B., Ramelli, A.R., 1991. Historical surface faulting in the Basin and Range province, western North America: implication for fault segmentation. Journal of Structural Geology 13, 123–136.

Doust, H., Omatsola, E., 1990. Niger Delta. In: Edwards, J.D., Santogrossi, P.A. (Eds.), Divergent/Passive Margin Basins. AAPG Memoir 48, pp. 201–238.

Dreyer, W., 1982. Underground Storage of Oil and Gas in Salt Deposits and Other Non-hard Rocks. F. Enke Verlag, Stuttgart.

Etchecopar, A., Granier, T., Larroque, J.M., 1986. Origine des fentes en échelon: propagation des failles. Comptes rendus de l'Académie des Sciences de Paris 302, 479–484.

Faure, J.L., Chermette, J.C., 1989. Deformation of tilted blocks, consequences on block geometry and extension measurements. Bulletin de la Société géologique de France 8, 461–476.

Gauthier-Lafaye, F., 1986. Les gisements d'uranium du Gabon et les réacteurs d'Oklo: modèle métallogènique de gîtes à fortes teneurs du Protérozoïque inférieur. Sciences Géologiques 78, 1–203.

Gauthier-Lafaye, F., Weber, F., 1989. The Francevillian (lower Proterozoic) uranium ore deposits of Gabon. Economic Geology 84, 2267–2285.

Gross, M.R., Gutierrez-Alonzo, G., Bai, T., Wacker, M.A., Collins-Worth, K.B., Behl, R.J., 1997. Influence of mechanical stratigraphy and kinematics on fault scaling relations. Journal of Structural Geology 19, 171–183.

Hancock, P.L., Barka, A.A., 1987. Kinematic indicators on active normal faults in western Turkey. Journal of Structural Geology 9, 573–584.

Hancock, P.L., Yeats, R.S., Sanderson, D.J. (Eds.), 1991. Characteristics of Active Faults. Journal of Structural Geology 13 (2).

Huggins, P., 1996. Normal fault segmentation and surface continuity: lithological control on fault growth, fault zone structure and seal potential. In: Jones, G., Fisher, Q., Knipe, R.J. (Eds.). Faulting, Fault Sealing and Fluid Flow in Hydrocarbon Reservoirs. Abstracts of Proceedings. University of Leeds, pp. 102–103.

Huggins, P., Watterson, J., Walsh, J.J., Childs, C., 1995. Relay zone geometry and displacement transfer between normal faults recorded in coalmine plans. Journal of Structural Geology 17, 1741–1755.

Jackson, J.A., White, N.J., 1989. Normal faulting in the upper continental crust: observations from regions of active extension. Journal of Structural Geology 11, 15–36.

Kattenhorn, S.A., Aydin, A., Pollard, D.D., 2000. Joints at high angles to normal fault strike: an explanation using 3-D numerical models of fault-perturbed stress fields. Journal of Structural Geology 22, 1–23.

Knipe, R.J., Jones, G., Fisher, Q.J., 1998. Faulting, fault sealing and fluid flow in hydrocarbon reservoirs: an introduction. In: Jones, G., Fisher, Q.J., Knipe, R.J. (Eds.), Faulting, Fault Sealing and Fluid Flow in Hydrocarbon Reservoirs. Geologycal Society Special Publications 147, pp. vii–xxi.

Larsen, P.H., 1988. Relay structures in a Lower Permian basement-involved extension system, East Greenland. Journal of Structural Geology 10, 3–8.

Laubach, S.E., Vendeville, B.C., Reynolds, S.J., 1992. Patterns in the development of extensional fault-block shapes from comparison of outcrop-scale faults and experimental physical models. In: Larsen, R.M., Brekke, H., Larsen, B.T., Talleraas, E. (Eds.), Structural and Tectonics Modelling and its Application to Petroleum Geology. Norwegian Petroleum Society Special Publication 1, pp. 231–241.

McGrath, A.G., Davison, I., 1995. Damage zone geometry around fault tips. Journal of Structural Geology 17, 1011–1024.

Machette, M.N., Personius, S.F., Nelson, A.R., Schwartz, D.P., Lund, W.R., 1991. The Wasatch fault zone, Utah—segmentation and history of Holocene earthquakes. Journal of Structural Geology 13, 137–149.

Maerten, L., Willemse, E.J.M., Pollard, D.D., Rawnsley, K., 1999. Slip distributions on intersecting normal faults. Journal of Structural Geology 21, 259–271.

Mansfield, C.S., Cartwright, J.A., 1996. High resolution fault displacement mapping from three-dimensional seismic data: evidence for dip linkage during fault growth. Journal of Structural Geology 18, 249–263.

Marchal, D., 1997. Approche spatio-temporelle des mécanismes de la propagation des failles normales: des modélisations analogiques à la sismique 3D. Ph.D. thesis, Université Henry Poincaré-Nancy I.

Marchal, D., Guiraud, M., Rives, T., Van Den Driessche, J., 1998. Space and time propagation processes of normal faults. In: Jones, G., Fisher, Q.J., Knipe, R.J. (Eds.), Faulting, Fault Sealing and Fluid Flow in Hydrocarbon Reservoirs. Geological Society Special Publications 147, pp. 51–70.

Morley, C.K., Nelson, R.A., Patton, T.L., Munn, S.G., 1990. Transfer zones in the East African rift system and their relevance to hydrocarbon exploration in rifts. American Association of Petroleum Geologists Bulletin 74, 1234–1253.

Needham, T., Yielding, G., Freeman, B., 1996. Analysis of fault geometry and displacement patterns. In: Buchanan, P.G., Nieuwland, D.A. (Eds.), Modern Development in Structural Interpretation, Validation and Modelling. Geological Society Special Publications 199, pp. 189–199.

Nicol, A., Watterson, J., Walsh, J.J., Childs, C., 1996. The shapes, major axis orientations and displacement patterns of fault surfaces. Journal of Structural Geology 18, 235–248.

Peacock, D.C.P., Sanderson, D.J., 1991. Displacements, segment linkage and relay ramps in normal fault zones. Journal of Structural Geology 13, 721–733.

Peacock, D.C.P., Sanderson, D.J., 1994. Geometry and development of relay ramps in normal fault systems. American Association of Petroleum Geologists Bulletin 78, 147–165.

Peacock, D.C.P., Zhang, X., 1994. Field examples and numerical modelling of oversteps and bends along normal faults in cross-section. Tectonophysics 234, 147–167.

Petit, J.-P., Barquins, M., 1988. Can natural faults propagate under mode II conditions?. Tectonics 7, 1243–1256.

Petit, J.-P., Barquins, M., 1993. Localisation des bandes de cisaillement par un défaut isolé préexistant: données expérimentales. Bulletin de la Société géologique de France 164, 255–266.

Pollard, D.D., Segall, P., Delaney, P.T., 1982. Formation and interpretation of dilatant échelon cracks. Geological Society of America Bulletin 93, 1291–1303.

Rawnsley, K.D., Peacock, D.C.P., Rivos, T., Petit, J.-P., 1998. Joints in the Mesozoic sediments around the Bristol Channel Basin. Journal of Structural Geology 20, 1641–1661.

Rippon, J.H., 1985. Contoured patterns of the throw and hade of normal faults in the Coal Measures (Westphalian) of north-east Derbyshire. Proceedings of the Yorkshire Geological Society 45, 147–161.

Roberts, A.M., Yielding, G., Freeman, B. (Eds.), 1991. The Geometry of Normal Faults. Geological Society Special Publication 56.

Schlische, R.W., Young, S.S., Ackermann, R.V., Gupta, A., 1996. Geometry and scaling relations of a population of very small rift-related normal faults. Geology 24, 683–686.

Shelton, J.W., 1984. Listric normal faults: an illustrated summary. American Association of Petroleum Geologists Bulletin 68, 801–815.

Stewart, I.S., Hancock, P.L., 1991. Scales of structural heterogeneity within neotectonic normal fault zones in the Aegean region. Journal of Structural Geology 13, 191–204.

Trudgill, B., Cartwright, J., 1994. Relay-ramp forms and normal-fault linkages, Canyonlands National Park, Utah. Geological Society of America Bulletin 106, 1143–1157.

Vendeville, B., 1991. Mechanisms generating normal fault curvature: a review illustrated by physical models. In: Roberts, A., Yielding, G., Freeman, B. (Eds.), Geometry of Normal Faults. Geological Society Special Publication 56, pp. 241–249.

Walsh, J.J., Watterson, J., 1989. Displacement gradients on fault surfaces. Journal of Structural Geology 11, 307–316.

Walsh, J.J., Watterson, J., 1991. Geometric and kinematic coherence and scale effects in normal fault systems. In: Roberts, A.M., Yielding, G., Freeman, B. (Eds.), Geometry of Normal Faults. Geological Society Special Publication 56, pp. 193–203.

Willemse, E.J.M., 1997. Segmented normal faults: correspondence between three-dimensional mechanical models and field data. Journal of Geophysical Research 102, 675–692.

Willemse, E.J.M., Pollard, D.D., Aydin, A., 1996. Three-dimensional analyses of slip distributions on normal fault arrays with consequenses for fault scaling. Journal of Structural Geology 18, 295–309.

Wu, D., Bruhn, R.L., 1994. Geometry and kinematics of active normal faults, South Oquirrh Mountains, Utah: implication for fault growth. Journal of Structural Geology 16, 1061–1075.

Yeats, R.S., Sieh, K., Allen, C.R., 1997. The Geology of Earthquakes. Oxford University Press.

Zhang, P., Slemmons, D.B., Mao, F., 1991. Geometric pattern, rupture termination and fault segmentation of the Dixie Valley active normal fault system, Nevada, USA. Journal of Structural Geology 13, 165–176.